Bichromatic dressing of Rydberg atoms and on the correctness of many-mode Floquet theory

by

Adam Poertner

A thesis
presented to the University of Waterloo
in fulfillment of the
thesis requirement for the degree of
Master of Science
in
Physics

Waterloo, Ontario, Canada, 2020

Author's Declaration

I hereby declare that I am the sole author of this thesis. This is a true copy of the thesis, including any required final revisions, as accepted by my examiners.

I understand that my thesis may be made electronically available to the public.

Abstract

Many-mode Floquet theory [T.-S. Ho, S.-I. Chu, and J. V. Tietz, Chem. Phys. Lett. **96**, 464 (1983)] was designed as an extension of Floquet theory suitable for solving the time-dependent Schrödinger equation with multiple periodicities, however its limitations are not well understood. I show that for two commensurate frequencies (integer multiples of a common frequency), many-mode Floquet theory always produces an exact expression for the time evolution of a system, despite only part of the eigenvalue spectrum being directly relevant. I show that the rest of the spectrum corresponds to eigenvalues of the same system but at other values of the relative phase between the bichromatic field components.

I show by using a Floquet perturbative analysis that dressing a Rydberg atom with a bichromatic field with frequency components ω_2 and ω_1, such that $\omega_2 = 2\omega_1$, can induce a permanent dipole moment (first order energy shift with dc electric field) without a dc bias field. With frequency $\omega_1 = 2\pi \cdot 5.997$GHz, $\omega_2 = 2\omega_1$ and field strengths of $E_{ac_1} = 0.1$ V/cm and $E_{ac_2} = 0.05$ V/cm, a permanent dipole moment of magnitude 44.06 MHz/(V/cm) is induced in the dressed $65s_{1/2}$ state of ^{85}Rb. The permanent dipole moment depends on the relative phase between the fields and can be made to be zero at certain values of phase.

Acknowledgements

I would like the thank all of the people who have made this thesis possible. First, I would like to thank my advisor, James Martin for all of your help over the past two years. Your never-ending patience and willingness to help will always be appreciated. This thesis would not have been possible without you.

I would like to thank the members of examination committee, Kyung Soo Choi and Pierre-Nicholas Roy, for their time and helpful comments. I also thank Kyung Soo Choi and Michal Bajcsy for acting as my advisory committee.

I thank Alexandre Cooper-Roy and Nadine Fladd for their helpful comments on Chapter 2 of this thesis.

Lastly, I would like to thank all of my friends and family for their support. In particular, my parents — Lorna and Peter — thank you for your continued support and everything else you have done for me.

Table of Contents

List of Tables

List of Figures

Chapter 1

Introduction

The dressing of Rydberg atoms by microwave fields in this work was originally inspired by Booth *et al.* [1] who used two ac electric fields (hereafter referred to as a bichromatic field) to show that *polarizability nulling* (to be discussed in more detail in Section 3.2.3) is possible in Rydberg states of Cesium. Rydberg atoms have found recent use in neutral atom qubits [2, 3] which rely on the *Rydberg blockade* interaction [4]. Details regarding implementation of neutral atom qubits will not be discussed here, other than to note that the Rydberg blockade relies on strong dipole-dipole interactions between Rydberg atoms. Polarizability nulling, if implemented correctly, would aid in the stabilization of the qubits by reducing their sensitivity to stray dc electric fields [1].

In Ref. [1], the dressing of Rydberg atoms was analyzed using *many-mode Floquet theory* [5] — an extension of Floquet theory which is designed specifically to handle two (or more) ac fields. While examining the justification of many-mode Floquet theory (both in the original paper and subsequent publications), it was evident that it has limitations that are not well understood, and in fact concerns have been raised in the literature [6, 7, 8] regarding its validity.

In Chapter 2, I discuss these concerns in detail and offer resolution through a comparison of many-mode Floquet theory to Shirley's Floquet theory [9], which is known to give exact results for periodic time-dependence. I show that (for commensurate frequencies) many-mode Floquet theory always provides the correct time-evolution of the system despite only part of the many-mode eigenvalue spectrum having direct relevance to the system in question. I then offer a physical interpretation of the remainder of the spectrum.

After resolving the issues with many-mode Floquet theory, I return to analyze the dressing of a Rydberg atom with a bichromatic field. While my original intention was

to demonstrate polarizability nulling in Rubidium, after analyzing this problem from a Floquet perturbative standpoint, I found that a permanent electric dipole moment can be induced by using a bichromatic field *without* the use of a dc electric field. Having found no work in the literature regarding the use of a bichromatic field (and zero-dc field) to induce a permanent dipole moment in a Rydberg atom[1], I chose to focus on this aspect of bichromatic dressing rather than polarizability nulling[2].

Inducing a permanent electric dipole moment in a Rydberg atom can increase the strength of the dipole-dipole interactions necessary for neutral atom qubits. However, rather than using a dc electric field, a bichromatic field has potential benefits which include the ability to produce a permanent dipole moment more quickly[3], or in situations where applying dc fields is difficult (for example, some experiments involving Rydberg atoms rely on glass cells which largely prevent the application of external dc fields. See, for example, [10]).

In Chapter 3, I show that the conditions that lead to the asymmetry of a bichromatic field also lead to an induced permanent dipole moment in an atom. I then offer the result of calculations regarding the dressing of a Rydberg state in Rubidium with an electric field with frequency components $\omega_2 = 2\omega_1$. Chapter 3 can be read independently of Chapter 2 as long as the reader is familiar with Floquet theory (which is reviewed in Section 2.2.2).

For clarification purposes — in this work, a permanent dipole moment[4] induced by a bichromatic field only refers to a first-order (linear) energy shift due to a dc electric field around 0V/cm.

[1] Any work in the literature regarding the use of a bichromatic field to induce a permanent dipole moment in molecules or atoms other than Rydberg states is not discussed. I only focus on Rydberg atoms in this work.

[2] I do not completely abandon polarizability nulling, as I show in Section 3.2.3 that it can potentially be used in conjunction with inducing a permanent dipole moment.

[3] That turning on a bichromatic field is quicker than producing a dc electric field is typically an observed experimental effect, however is not necessarily strictly true.

[4] I will only be considering electric dipole moments.

Chapter 2

Many-mode Floquet theory with commensurate frequencies

This chapter focuses on many-mode Floquet theory. The material in this chapter is directly based on a paper I have co-authored with James Martin [11].

2.1 Introduction

In quantum mechanics there is hardly a task more fundamental than solving the time-dependent Schrödinger equation. A particularly important case is atomic evolution in the presence of classically prescribed electromagnetic fields, corresponding to Hamiltonians of the form: $H(t) = H_0 + V(t)$, where the time-independent H_0 describes the atomic system in the absence of the fields, and a (possibly) time-varying $V(t)$ accounts for the presence of the fields.

The frequent situation that the fields are periodic in time may be deftly handled using Floquet theory: suppose that there is a single relevant time-dependent field, periodic in time, so that $V(t) = V(t+T)$ for some period T and for all times t. If a finite basis of dimension N_A may be used to describe the atomic system, Floquet theory tells us that there are N_A independent solutions for the state vector of the form [9]:

$$|\psi_j(t)\rangle = e^{-iE_j t/\hbar} |\phi_j(t)\rangle \,, \tag{2.1}$$

where we have labelled each of the solutions with index j. The E_j's are known as the *quasi-energies* and the corresponding $|\phi_j(t)\rangle$'s — so-called *quasi-states* — have the same

periodicity as the Hamiltonian: $|\phi_j(t)\rangle = |\phi_j(t+T)\rangle$. This periodicity suggests a Fourier expansion:

$$|\phi_j(t)\rangle = \sum_n |\tilde{\phi}_j(n)\rangle\, e^{in\omega t} \tag{2.2}$$

where $\omega = 2\pi/T$. Shirley [9] showed that when the time-dependent Schrödinger equation (TDSE) is expressed in terms of the $|\tilde{\phi}_j(n)\rangle$ expansion "coefficients", all N_A of the solutions — in form of Eq. 2.1 — may be determined from the eigenstates and energies of a *time-independent* matrix (the "Floquet" Hamiltonian). Once all of the solutions are known, it is straightforward to write the unitary time evolution operator, constituting a complete solution for the quantum mechanical evolution of the atomic system in the presence of the periodic field.

In addition to having a certain aesthetic appeal, Shirley's formulation of Floquet theory (SFT) is often well-suited for explicit computations, as it may just involve a straightforward generalization of a simpler time-independent problem (for an example in Rydberg atom physics see Ref. [12]).

Here we are concerned with a generalization of SFT to two (or more) fields of *different* periodicities; for example, $H(t) = H_0 + V_1(t) + V_2(t)$ where $V_1(t) = V_1(t+T_1)$ and $V_2(t) = V_2(t+T_2)$ for all t, and $T_1 \neq T_2$. If the ratio of the corresponding frequencies $f_1 = 1/T_1$ and $f_2 = 1/T_2$ may be represented as: $f_1/f_2 = N_1/N_2$ where N_1 and N_2 are integers — so-called *commensurate* frequencies — a period common to both $V_1(t)$ and $V_2(t)$ exists ($T = N_1/f_1 = N_2/f_2$). Thus this situation is completely handled by SFT, albeit awkwardly — the couplings due to each of the fields are at (different) harmonics of the common base frequency $1/T$, the details depending on N_1 and N_2.

As an alternative, Ho *et al.* [5] extended SFT in a way that removes explicit references to N_1 and N_2, thereby recovering the elegance and simplicity of SFT for a field of a single periodicity. In a similar manner to SFT, this formulation involves a unitary time evolution operator written in terms of a *time-independent* many-mode Floquet theory (MMFT) Hamiltonian.

The MMFT formulation has been used for nuclear magnetic resonance [13], dressed potentials for cold atoms [14], microwave dressing of Rydberg atoms [1], and superconducting qubits [15], to name but a few examples. Nonetheless, independent groups have questioned the validity of MMFT [7, 8] and the completeness [6] of the justification of MMFT given in Ref. [5]. Subsequent publications [16, 17] by one of the authors of the original MMFT paper [5] support the conjecture [7] that the MMFT formulation is approximately correct in some commensurate cases, but is entirely correct for incommensurate cases (irrational

frequency ratios), in dissonance with the justification presented in Ref. [5] which is based on commensurate frequencies.

Prompted by the recent use of MMFT in a Rydberg atom study [1], we began to consider its correctness, particularly for two commensurate frequencies described by low N_1 and N_2, which are often relatively easy to simultaneously generate in an experiment (i.e. as low harmonics of a common frequency source). We computed the time evolution of a simple system in the case of commensurate frequencies numerically using MMFT and compared our results to both SFT and direct integration of the TDSE and were surprised to find no differences (when adequate basis sizes, time steps, etc. were chosen). This agreement is at apparent odds with the literature questioning the general applicability of MMFT and our own expectations after examination of the justification of MMFT given in Ref. [5]. We found this situation confusing, to say the least.

In this work, we resolve these discrepancies by showing that MMFT may be used to correctly compute time evolution, *and that this is consistent with* the fact that not all of the eigenpairs[1] of the MMFT Hamiltonian correspond to the Floquet quasi-energies and quasi-states (i.e. the E_j's and $|\phi_j(t)\rangle$'s of Eq. 2.1).

The case of incommensurate frequencies (see, for example, Ref.'s [18] and [19]) is beyond the scope of this work.

Many readers will be familiar with the background on Shirley's formulation of Floquet theory (SFT) [9] that we review in Section 2.2.1, but perhaps less so with Ho *et al.'s* [5] MMFT theory, as reviewed in Section 2.2.3. We include these sections for completeness and to establish notation. Our results are in Section 2.3, where we show how the SFT and MMFT approaches may be considered to be equivalent, and address the concerns with MMFT raised in the literature [7, 8, 6]. Section 2.4 concludes with a summary and a discussion of the utility of MMFT in the case of commensurate frequencies.

2.2 Background

2.2.1 Floquet theory

As a foundation for discussion of the multiple-frequency case, this section reviews Floquet theory as it applies to the solution of the TDSE:

$$i\hbar\frac{d}{dt}|\psi(t)\rangle = \hat{H}(t)|\psi(t)\rangle \tag{2.3}$$

[1] We refer to an eigenvector and its associated eigenvalue collectively as an *eigenpair*.

given a Hamiltonian that is both periodic $\hat{H}(t) = \hat{H}(t+T)$ and Hermitian $\hat{H}^\dagger(t) = \hat{H}(t)$ for all times t. To simplify — but not restrict the results in a fundamental way — the state vectors $|\psi(t)\rangle$ will be considered as belonging to a finite-dimensional inner-product space A of dimension N_A. In what follows this shall be referred to as the *atomic space*.

Since the Hamiltonian is Hermitian, we may define a unitary time evolution operator $\hat{U}(t_2, t_1)$ satisfying

$$|\psi(t_2)\rangle = \hat{U}(t_2, t_1)\,|\psi(t_1)\rangle \tag{2.4}$$

for all t_1 and t_2.

Floquet theory is slightly more general than required here — the general theory is not restricted to unitary time evolution (see, for example, Ref. [20]). For the unitary case, Floquet theory implies (see, for example, Ref. [21]) that the quasi-states of Eq. 2.1 exist and may be combined to give:

$$\hat{U}(t, 0) = \sum_{j=1}^{N_A} |\phi_j(t)\rangle\, e^{-iE_j t/\hbar}\, \langle\phi_j(0)|\,. \tag{2.5}$$

The quasi-energies and corresponding quasi-states may be determined from $\hat{U}(T, 0)$ as obtained by direct numerical integration of the TDSE over the duration of a single period T (see, for example, Ref. [22]). However, SFT and MMFT provide an alternate approach to direct integration, introduced by Shirley [9], and discussed in the next section.

2.2.2 Shirley's formulation of Floquet theory (SFT)

The SFT Hamiltonian

The use of Fourier decomposition to find Floquet-type solutions (e.g. Eq. 2.2) has a long history, originating with Hill's theory regarding the motion of the moon (see, for example, Ref. [23]). Following earlier more specific work by Autler and Townes [24], Shirley [9] applied these ideas to the unitary time evolution of quantum mechanics, showing that determination of the quasi-energies and quasi-states reduces to a linear eigenvalue problem similar to the normal eigenvalue problem $\hat{H}\,|\psi\rangle = E\,|\psi\rangle$ for *time-independent* Hamiltonians. In this section, we reproduce Shirley's Floquet theory (SFT) using a slightly modified notation suitable for extension to MMFT (similar in spirit to that of Ref. [25]).

Consider an infinite-dimensional inner-product space F for Fourier decomposition, spanned by an orthonormal basis set: $\{|n\rangle_F \mid n \in \mathbb{Z}\}$, where $\mathbb{Z}$ refers to the set of all

integers and $\langle m|n\rangle_F = \delta_{m,n}$. The full time-dependence of the quasi-states of Eq. 2.2 will be represented using a time-dependent superposition of *time-independent* vectors from the tensor product space $F \otimes A$:

$$|\phi_j(t)\rangle_A = \sum_{n=-\infty}^{\infty} e^{in\omega t} \left[\langle n|_F \otimes \hat{I}_A\right] |\phi_j\rangle_{F\otimes A} \tag{2.6}$$

where $\hat{I}_A$ is the identity in the atomic space A. (Hitherto all operators and vectors were in the atomic space; henceforth we will be explicit, and for clarity avoid referring to vectors in $F \otimes A$ as "states".)

Vectors in $F \otimes A$ may be decomposed using the basis sets for F and A:

$$|\phi_j\rangle_{F\otimes A} = \sum_{m,\alpha} D_j(m,\alpha)\ |m\rangle_F \otimes |\alpha\rangle_A\,, \tag{2.7}$$

where the expansion coefficients $D_j(m,\alpha)$ are complex numbers, and here and after summations over Fourier indices are implicitly from $-\infty$ to ∞.

We may determine the quasi-energies and expansion coefficients for a specific problem by substitution of

$$|\psi_j(t)\rangle_A = e^{-iE_jt} \sum_n e^{in\omega t} \left[\langle n|_F \otimes \hat{I}_A\right] |\phi_j\rangle_{F\otimes A} \tag{2.8}$$

into the TDSE (Eq. 2.3 with $\hbar = 1$ and hereafter) and Fourier expanding the Hamiltonian: $\hat{H}_A(t) = \sum_m \tilde{H}_A(m)e^{im\omega t}$. The result [9] is a linear eigenvalue problem:

$$\hat{H}_{F\otimes A}\,|\phi_j\rangle_{F\otimes A} = E_j\,|\phi_j\rangle_{F\otimes A} \tag{2.9}$$

where the *Floquet Hamiltonian* $\hat{H}_{F\otimes A}$ is:

$$\hat{H}_{F\otimes A} \equiv \sum_n \left\{n\omega\,|n\rangle\,\langle n|_F \otimes \hat{I}_A\right\} + \sum_m \left\{\hat{S}_F(m) \otimes \tilde{H}_A(m)\right\}, \tag{2.10}$$

where the "shift operators" are defined as:

$$\hat{S}_F(m) \equiv \sum_n |n+m\rangle\,\langle n|_F\,. \tag{2.11}$$

The original time-dependent problem has now been formulated as a familiar *time-independent* eigenvalue problem by which the quasi-energies E_j's and expansion coefficients (the $D_j(m,\alpha)$'s in Eq. 2.7) may be determined.

Since there are an infinite number of Fourier coefficients, the matrix representation of $\hat{H}_{F\otimes A}$ is infinite, reflecting a superfluity associated with the quasi-states and quasi-energies: if we shift a quasi-energy by $\hbar\omega$ — or equivalently by ω in the simplified units of this section — this may be compensated for by simultaneously shifting the corresponding expansion coefficients, so as to describe the same solution. i.e. we may combine Eq.'s 2.7 and 2.8 to give:

$$|\psi_j(t)\rangle_A = e^{-iE_{j,p}t} \sum_{m,\alpha} e^{im\omega t} D_j(m-p,\alpha)\,|\alpha\rangle_A \tag{2.12}$$

where $E_{j,p} \equiv E_j + p\omega$ with p *any* integer. (By convention we may choose $-\omega/2 < E_j \leq \omega/2$ for all j.) The corresponding shifted eigenvectors of $\hat{H}_{F\otimes A}$ are given by

$$|\phi_{j,p}\rangle_{F\otimes A} \equiv \left[\left(\sum_\ell |\ell+p\rangle\,\langle\ell|_F\right)\otimes \hat{I}_A\right] |\phi_j\rangle_{F\otimes A}\,. \tag{2.13}$$

Examination of $\hat{H}_{F\otimes A}$ shows that if E_j and $|\phi_j\rangle$ are an eigenpair then so are $E_{j,p}$ and $|\phi_{j,p}\rangle$.

Thus, although matrix representations of $\hat{H}_{F\otimes A}$ are infinite (due to the F space), there are really only N_A non-trivially distinct eigenpairs, which is consistent with the finite summation of Eq. 2.5. In practice, estimates of the spectrum of $\hat{H}_{F\otimes A}$ may be obtained through diagonalization in a truncated, finite basis, as will be illustrated by an example in Section 2.2.2.

The SFT propagator

Shirley [9] showed that it is possible to express the matrix elements of the unitary time evolution operator using the Floquet Hamiltonian $\hat{H}_{F\otimes A}$ directly, without explicit reference to the quasi-energies and states:

$$\langle\beta|\hat{U}_A(t,0)|\alpha\rangle_A = \sum_n e^{in\omega t}\left[\langle n|_F \otimes \langle\beta|_A\right] e^{-i\hat{H}_{F\otimes A}t}\left[|0\rangle_F \otimes |\alpha\rangle_A\right]. \tag{2.14}$$

Although α and β represent arbitrary atomic states, in a slight abuse of terminology we will refer this expression as a *propagator*. It follows from the insertion of the form for $|\phi_j(t)\rangle_A$ given by Eq. 2.6 into the expression for the unitary time evolution operator given by Eq. 2.5. Together with the definition of the SFT Hamiltonian (Eq. 2.10) it encapsulates all of SFT, and thus will serve as a useful means by which to compare SFT and MMFT.

Example of the usage of SFT

To illustrate our main points regarding the correctness of MMFT we will consider computation of the time evolution of an atomic system with a Hamiltonian consisting of two periodic, commensurate couplings. In this section we look at a specific example using SFT, and will return to the same example using MMFT in Sections 2.2.3 and 2.3.3. Our particular choice of system is simple and subfield-agnostic, but otherwise is somewhat arbitrary. (Although we are ultimately interested in bichromatic microwave dressing of Rydberg atoms [1], that is not relevant here. And although we choose frequencies such that $N_1 = 1$ and $N_2 = 2$, other choices, such as $N_1 = 2$ and $N_2 = 3$, would also illustrate our points.)

The atomic system is described using an orthonormal basis consisting of two states, lower (ℓ) and upper (u), evolving according to the TDSE (Eq. 2.3) with the Hamiltonian:[2]

$$\begin{aligned}\hat{H}_A(t) = E_u \left|u\right\rangle \left\langle u\right|_A + E_\ell \left|\ell\right\rangle \left\langle \ell\right|_A + 2V \left(\cos(\omega t) + \cos(2\omega t + \phi_{2\omega})\right) \\ \times \left(\left|u\right\rangle \left\langle l\right|_A + \left|l\right\rangle \left\langle u\right|_A\right)\end{aligned} \tag{2.15}$$

where $E_u = 3/2$, $E_\ell = 0$, $\omega = 1$, $V = 1$ and $\hbar = 1$. We will study this $\omega, 2\omega$ with different values of the phase $\phi_{2\omega}$, as it turns out to be significant in the comparison of SFT and MMFT.

With such a small atomic space ($N_A = 2$) it is straightforward to directly integrate the TDSE with the Hamiltonian of Eq. 2.15, using standard numerical methods, without any consideration of Floquet theory. Starting with all the population in ℓ at $t = 0$, Fig. 2.1a) illustrates the computed time evolution for two values of the phase $\phi_{2\omega}$.

This time evolution may also be computed using the SFT propagator of Eq. 2.14, where the plotted quantity in Fig. 2.1a) is $\left|\left\langle u\right| \hat{U}_A(t) \left|\ell\right\rangle_A\right|^2$. For $\hat{H}_{F\otimes A}$ we use Eq. 2.10, with

$$\tilde{H}_A(0) = E_u \left|u\right\rangle \left\langle u\right|_A + E_\ell \left|\ell\right\rangle \left\langle \ell\right|_A \tag{2.16a}$$

$$\tilde{H}_A(\pm 1) = V(\left|u\right\rangle \left\langle l\right|_A + \left|l\right\rangle \left\langle u\right|_A) \tag{2.16b}$$

$$\tilde{H}_A(\pm 2) = V e^{\pm i\phi_{2\omega}}(\left|u\right\rangle \left\langle l\right|_A + \left|l\right\rangle \left\langle u\right|_A), \tag{2.16c}$$

and all other couplings zero.

The $F \otimes A$ space of SFT is infinite-dimensional due to the Fourier decomposition space F. To numerically evaluate Eq. 2.14 we truncate the standard basis for F. Instead of

[2]The unperturbed energy level splitting $E_u - E_\ell$ results in "equal and opposite" detunings of ω and 2ω, and is inspired by Ref. [26], but is of no special significance to our main points.

summation over all integer n, only a finite set is considered: $\mathcal{N} = \{n \in \mathbb{Z} \mid n_{\min} \leq n \leq n_{\max}\}$: the basis for $F \otimes A$ being formed from the tensor product of the vectors for F from $\mathcal{B}_F = \{|n\rangle_F \mid n \in \mathcal{N}\}$ and the basis vectors for the atomic space. The size of the basis is $N_{\mathcal{B}_F} \times N_A$ where $N_{\mathcal{B}_F}$ refers to the number of elements in $\mathcal{B}_F$. A finite matrix version of $\hat{H}_{F\otimes A}$ is considered by simply ignoring couplings between vectors not described by this finite basis. This finite-dimensional version of $\hat{H}_{F\otimes A}$ is diagonalized numerically and in place of $e^{-i\hat{H}_{F\otimes A}t}$ in Eq. 2.14, we use $\sum_j e^{-iE_j t} |\phi_j\rangle \langle\phi_j|_{F\otimes A}$ where j indices a complete set of eigenpairs of the finite $\hat{H}_{F\otimes A}$.

If for simplicity[3] we select $\mathcal{B}_F$'s with $n_{\min} = -n_{\max}$, then $n_{\max} \geq 10$ is necessary for the finite matrix version of Eq. 2.14 to compute $\left|\langle u| \hat{U}_A(t) |\ell\rangle_A\right|^2$ at $t = 2\pi$ to within 10^{-2} for $\phi_{2\omega} = 0$.

Figure 2.1b) shows a finite portion of the computed quasi-energy spectrum (the eigenvalues of the finite $\hat{H}_{F\otimes A}$). As expected based on the discussion around Eq. 2.12 the quasi-energies repeat vertically in the figure with a periodicity of $\hbar\omega$ ($= 1$ for the simplified units of this example). (This property is approximate with a finite basis for F.)

Based on the significant difference in the time evolution observed in Fig. 2.1a) for the two values of $\phi_{2\omega}$ we might expect that the quasi-energy spectrum depends on $\phi_{2\omega}$. This is confirmed in part b) of the figure, where the quasi-energy spectrum is plotted as a function of $\phi_{2\omega}$ (by repeatedly diagonalizing the finite $\hat{H}_{F\otimes A}$ as $\phi_{2\omega}$ is varied).

This example may also be treated using MMFT, as discussed in the next section.

2.2.3 Many-mode Floquet theory (MMFT)

The MMFT Hamiltonian and propagator

For concreteness and correspondence with a common experimental scenario, consider an atomic system with dipole coupling to the electric field. With the superposition of two sinusoidal fields:

$$\hat{H}_A(t) = \tilde{H}_A(0) - \vec{\mu}_A \cdot \vec{E}_1 \cos(\omega_1 t + \phi_1) - \vec{\mu}_A \cdot \vec{E}_2 \cos(\omega_2 t + \phi_2). \tag{2.17}$$

As Leasure [27] pointed out and we have discussed in the introduction, if ω_1/ω_2 may be expressed as the ratio of two integers N_1/N_2 then such a Hamiltonian has a single

[3]This straightforward approach is not the most efficient means to numerically compute unitary time evolution using SFT. A more judicious choice of $\mathcal{B}_F$ and exploitation of the "repeated" nature of the spectrum would improve efficiency.

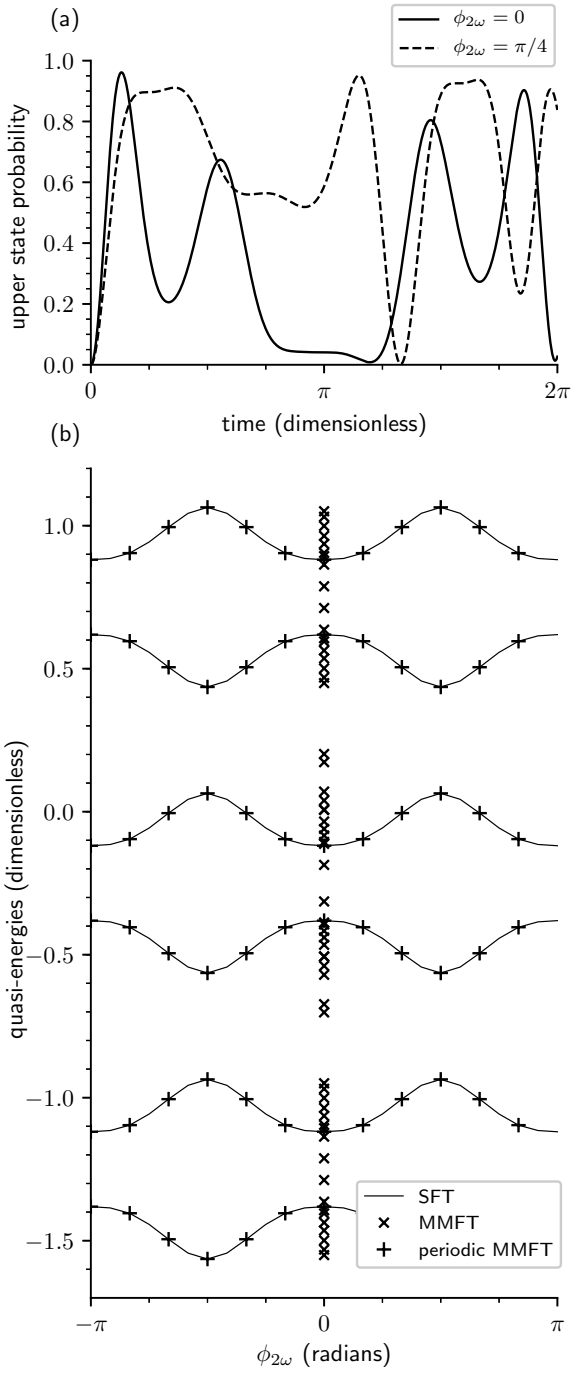

Figure 2.1: (a) Time evolution of the upper state population given the Hamiltonian of Eq. 2.15, with all population initially in the ground state. (b) Partial spectra for the same physical system as (a), computed by diagonalization of the SFT Hamiltonian with varying $\phi_{2\omega}$ ($-$ lines), computed by diagonalization of the MMFT Hamiltonian for $\phi_{2\omega} = 0$ ($\times$ points) as described in Section 2.2.3, and computed by diagonalization of the MMFT Hamiltonian using periodic boundary conditions ($+$ points) as described in Section 2.3.3.

periodicity.[4] With the common "base frequency" $\omega_B = \omega_1/N_1 = \omega_2/N_2$, the two time-dependent couplings in Eq. 2.17 are simply couplings at different harmonics of ω_B, so that we may Fourier expand:

$$\hat{H}_A(t) = \sum_m \tilde{H}_A(m) e^{im\omega_B t} \tag{2.18}$$

and thus the entire approach of Shirley [9] is applicable. (The example of Section 2.2.2 corresponds to $N_1 = 1$, $N_2 = 2$.)

Ho *et al.* [5] take this idea as their starting point for MMFT, and then consider "relabelling" Fourier basis vectors in Shirley's formulation as basis vectors from the tensor product of *two* Fourier spaces:

$$|n\rangle_F \xrightarrow{\text{relabel}} |n_1\rangle_{F_1} \otimes |n_2\rangle_{F_2}\,, \tag{2.19}$$

where $n\omega_B = n_1\omega_1 + n_2\omega_2$; or equivalently $n = n_1 N_1 + n_2 N_2$. We will discuss shortly whether or not this relabelling is possible for all n, and if so, if the choice of n_1 and n_2 is unique. In any case the new basis to be used consists of all possible integer n_1 and n_2's (in principle; in practice the basis is truncated using convergence criteria).

The paper introducing MMFT [5] focused on time-dependent Hamiltonians in the form of Eq. 2.17. Since then, the MMFT terminology has come to refer to a slightly more general situation in which the time-dependent Hamiltonians of interest have the form:

$$\hat{H}_A(t) = \sum_{p,q} \tilde{H}_A(p,q) e^{i(p\omega_1 + q\omega_2)t}. \tag{2.20}$$

for which Eq. 2.17 may be considered a special case (see the example of Section 2.2.3). We will focus on the two-mode[5] case for concreteness (see, for example, Ref. [13] for a many-mode generalization).

In this more general version of MMFT, the time-independent MMFT Hamiltonian in the new $F_1 \otimes F_2 \otimes A$ space is given as (with $\hbar = 1$):

$$\begin{aligned}\hat{H}_{F_1\otimes F_2\otimes A} = &\sum_{n_1,n_2} \left[n_1\omega_1 + n_2\omega_2\right] |n_1\rangle \langle n_1|_{F_1} \otimes |n_2\rangle \langle n_2|_{F_2} \otimes \hat{I}_A \\ &+ \sum_{p,q} \hat{S}_{F_1}(p) \otimes \hat{S}_{F_2}(q) \otimes \tilde{H}_A(p,q)\end{aligned} \tag{2.21}$$

[4] In all that follows we will assume that N_1 and N_2 are positive integers with a greatest common divisor of one.

[5] Depending on the context we will refer to the modes as *frequencies*, *fields*, or *couplings*, having in mind typical Hamiltonians of the form of Eq. 2.17. Arguably a more precise terminology for MMFT is *many-frequency Shirley Floquet theory*.

with the $\hat{S}_{F_1}$ and $\hat{S}_{F_2}$ shift operators defined by Eq. 2.11.

Ho *et al.* [5] generalize (but do not prove) the propagator due to Shirley [9] (our Eq. 2.14) to:

$$\begin{aligned}\langle\beta|\,\hat{U}(t,0)\,|\alpha\rangle = \sum_{n_1,n_2} e^{i[n_1\omega_1+n_2\omega_2]t}\left[\langle n_1|_{F_1}\otimes\langle n_2|_{F_2}\otimes\langle\beta|_A\right] \\ e^{-i\hat{H}_{F_1\otimes F_2\otimes A}t}\left[|0\rangle_{F_1}\otimes|0\rangle_{F_2}\otimes|\alpha\rangle_A\right].\end{aligned} \tag{2.22}$$

This expression appears again in the literature following Ho *et al.* [5], in, for example, Ref.'s [6, 15]. Both this propagator and the form of the MMFT Hamiltonian appear to be plausible generalizations of the analogous well-established results of SFT (Eq.'s 2.10 and 2.14). Furthermore, the MMFT Hamiltonian has the desirable property that no explicit references to N_1 and N_2 appear, so that its structure remains unchanged if ω_1 and ω_2 are varied. But we are not aware of a prior resolution of the issues that we discuss in the next section.

Concerns with the validity of MMFT

As mentioned in the introduction, concerns have been raised regarding the validity of MMFT [7, 8]. One troubling aspect of Ho et al.'s [5] justification for MMFT is the "relabelling" process (Eq. 2.19). Specifically, given any integer n, are there always integers n_1 and n_2 satisfying $n_1N_1 + n_2N_2 = n$, and if so, is the solution unique? Ho *et al.* [5] discuss existence but not uniqueness. Here we note that for a given rational ω_1/ω_2, the corresponding N_1 and N_2 can always be chosen so that their greatest common divisor $\gcd(N_1, N_2)$ is one. Thus there is *always* a solution (see, for example, Ref. [28]).[6] Moreover, there are an *infinite* number of solutions i.e. given one solution for integers n_1 and n_2 satisfying: $n = n_1N_1 + n_2N_2$, we also have:

$$\underbrace{(n_1+\ell N_2)}_{n_1'}N_1 + \underbrace{(n_2-\ell N_1)}_{n_2'}N_2 = n \tag{2.23}$$

for all integer ℓ, giving an infinite number of solutions (n_1' and n_2') (and also all possible solutions). Thus the relabelling process is not unique — basis states of different n_1 and n_2 can correspond to the same n, raising the question of over-completeness of the standard n_1, n_2 MMFT basis [7, 6]. We are not able to see any straightforward way to address this

[6] As such, $\gcd(N_1, N_2) = 1$ implies that only the $p = 0$ blocks of Ho *et al.* [5] are necessary (see the discussion following their Eq. 10). For this reason, we do not make use of their "p-block" construction. A related discussion appears in Ref. [6].

specific deficiency in Ho et al.'s [5] derivation, which has been characterized as incomplete [6].

A related issue is that for Hamiltonians like Eq. 2.17 it has been pointed out that the eigenvalues of the MMFT Hamiltonian do not depend on the relative phase of the two fields [8] (we detail this argument later in Section 2.3.2). Our example in Section 2.2.2 and Fig. 2.1 shows that this independence is problematic, as the quasi-energies obtained from SFT clearly *do* depend on $\phi_{2\omega}$.

Although Ho *et al.* [5] provided a specific numerical example showing that MMFT reproduces the results of explicit time integration of the TDSE, the effective N_1 and N_2's were quite large (when considered in conjunction with coupling strengths). In this situation previous workers have described MMFT as being *approximately* correct (see, for example, Ref. [7]), as typical finite basis sets used would not contain any "repeated states".

However these favourable conditions are not present in our example $\omega, 2\omega$ system of Section 2.2.2. Surprisingly, the next section empirically illustrates that MMFT works.

Example of the usage of MMFT

The MMFT propagator can be numerically evaluated in an analogous manner as the SFT propagator, as was described in Section 2.2.2. The difference being that we need to truncate the basis for $F_1 \otimes F_2$, rather than for F. Thus in Eq. 2.22 we will take the summations of a finite set of n_1 and n_2's. Similarly, a finite version of $\hat{H}_{F_1 \otimes F_2 \otimes A}$ can be diagonalized numerically to evaluate the matrix elements of $e^{-i\hat{H}_{F_1 \otimes F_2 \otimes A} t}$.

The time evolution of the $\omega, 2\omega$ system of Section 2.2.2 may also be determined using MMFT, with $\omega_1 = 1$, $\omega_2 = 2$,

$$\tilde{H}_A(0,0) = E_u \left|u\right\rangle \left\langle u\right|_A + E_\ell \left|\ell\right\rangle \left\langle \ell\right|_A \tag{2.24a}$$

$$\tilde{H}_A(\pm 1,0) = V(\left|u\right\rangle \left\langle l\right|_A + \left|l\right\rangle \left\langle u\right|_A) \tag{2.24b}$$

$$\tilde{H}_A(0,\pm 1) = V e^{\pm i\phi_{2\omega}}(\left|u\right\rangle \left\langle l\right|_A + \left|l\right\rangle \left\langle u\right|_A) \tag{2.24c}$$

and all other couplings zero. We construct a finite basis for $F_1 \otimes F_2$ with basis kets of the form $\left|n_1\right\rangle_{F_1} \otimes \left|n_2\right\rangle_{F_2}$ for all n_1 and n_2 such that $n_1 \in \mathcal{N}$ and $n_2 \in \mathcal{N}$, with $\mathcal{N} = \{n \in \mathbb{Z} \mid -n_{\max} \leq n \leq n_{\max}\}$. See Fig. 2.2(a) for an example of a finite basis set with $n_{\max} = 2$.

We find that $n_{\max} \geq 9$ is necessary for the finite matrix version of Eq. 2.22 to compute $\left|\left\langle u\right| \hat{U}_A(t) \left|\ell\right\rangle_A\right|^2$ at $t = 2\pi$ to within 10^{-2} for $\phi_{2\omega} = 0$.

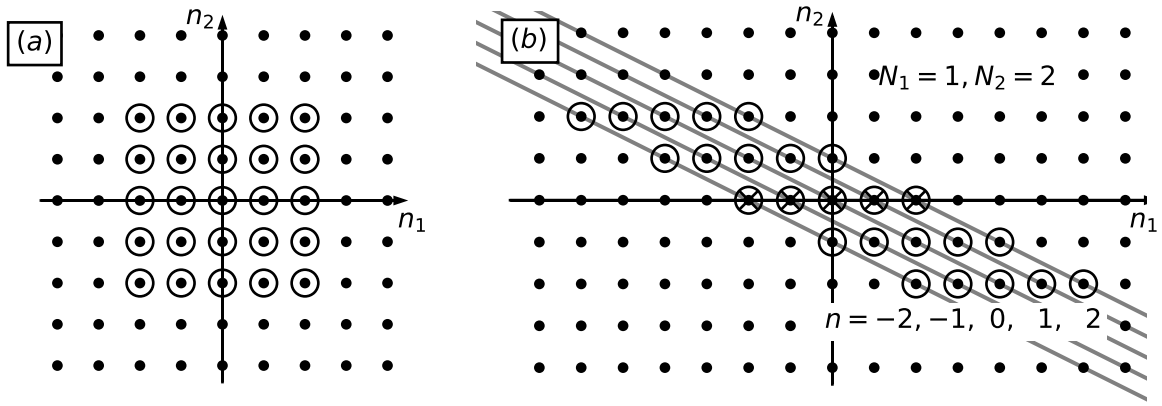

Figure 2.2: Finite basis sets for the $F_1 \otimes F_2$ space used in MMFT calculations. Points on the integer lattice ($\cdot$) represent basis vectors $|n_1\rangle_{F_1} \otimes |n_2\rangle_{F_2}$. In principle, basis sets for MMFT calculations should run over all integer n_1 and n_2; however finite basis sets ($\odot$) are typically used to numerically diagonalize MMFT Hamiltonians. Shown are: (a) a conventional choice (e.g. Ref. [5]), and (b) a basis set suitable for maintaining the "translational invariance" of the MMFT Hamiltonian (Eq. 2.26). The basis vector selection in (b) depends on N_1 and N_2 ($N_1 = 1$ and $N_2 = 2$ in this case). The lines connect basis vectors corresponding to the same n. The canonical vectors $|n_1(n)\rangle_{F_1} \otimes |n_2(n)\rangle_{F_2}$ for each n (see Appendix A) are indicated ($\otimes$).

That MMFT may accurately compute the time evolution in this system was a surprise to us given the concerns of the previous section and the nature of the eigenvalues of the finite basis MMFT Hamiltonian. Specifically, Fig. 2.1b) shows the eigenvalues for the truncated MMFT Hamiltonian with $\phi_{2\omega} = 0$ (the $\times$ points distributed vertically at $\phi_{2\omega} = 0$) illustrating that the spectrum of the MMFT Hamiltonian *does not* correspond to the SFT quasi-energies (solid line) at $\phi_{2\omega} = 0$. Despite this discrepancy, in numerical experimentation on a variety of commensurate systems (e.g. $2\omega, 3\omega$) we have found that Eq. 2.22 may be used to compute unitary time evolution.

2.3 The relationship of MMFT to SFT

2.3.1 Equivalence of the MMFT and SFT propagators

We will now show why calculations using the MMFT propagator given in Eq. 2.22 with the MMFT Hamiltonian of Eq. 2.21 are correct for commensurate frequencies, despite the concerns discussed in Section 2.2.3 and the discrepancy between the SFT and MMFT spectra noted in the previous section. We avoid the problematic relabelling procedure of Ho *et al.* [5] and take a rather different approach.

Specifically, we will exploit a symmetry of the MMFT Hamiltonian to help show the correctness of the MMFT propagator. Consider a unitary operator, that produces a "translated" version of a vector $|n_1\rangle_{F_1} \otimes |n_2\rangle_{F_2}$ corresponding to the same n ($\equiv n_1 N_1 + n_2 N_2$):

$$\hat{T}_{F_1 \otimes F_2} \equiv \hat{S}_{F_1}(N_2) \otimes \hat{S}_{F_2}(-N_1). \tag{2.25}$$

where the $\hat{S}$ operators are of the same form as Eq. 2.11. Defining $T_{F_1 \otimes F_2 \otimes A} \equiv \hat{T}_{F_1 \otimes F_2} \otimes \hat{I}_A$, it may be verified that the MMFT Hamiltonian given by Eq. 2.21 is invariant under this translation:

$$T^{-1}_{F_1 \otimes F_2 \otimes A} \hat{H}_{F_1 \otimes F_2 \otimes A} T_{F_1 \otimes F_2 \otimes A} = \hat{H}_{F_1 \otimes F_2 \otimes A}. \tag{2.26}$$

This symmetry suggests an analogy with the tight-binding Hamiltonians used for solid-state crystals, in which every lattice site has equivalent couplings to its neighbours (see, for example, Ref. [29]). In the case of MMFT with commensurate frequencies, the implications of this symmetry do not appear to have been fully explored (see, for example, the pedagogical treatment of MMFT in Ref. [30]).[7]

In particular, since $\hat{T}_{F_1 \otimes F_2 \otimes A}$ commutes with $\hat{H}_{F_1 \otimes F_2 \otimes A}$, if $|\psi\rangle_{F_1 \otimes F_2 \otimes A}$ is an eigenvector of $\hat{T}_{F_1 \otimes F_2 \otimes A}$ with eigenvalue e^{-ik}, with k real, then $\hat{H}_{F_1 \otimes F_2 \otimes A} |\psi\rangle_{F_1 \otimes F_2 \otimes A}$ is also an eigenvector of $\hat{T}_{F_1 \otimes F_2 \otimes A}$ with the same eigenvalue — the MMFT Hamiltonian does not "connect" eigenvectors of $\hat{T}_{F_1 \otimes F_2 \otimes A}$ corresponding to different eigenvalues. This suggests that we partially diagonalize $\hat{H}_{F_1 \otimes F_2 \otimes A}$ by replacing the n_1, n_2 basis for the $F_1 \otimes F_2$ space with one in which $\hat{T}_{F_1 \otimes F_2}$ is diagonal. We will refer to this new basis for the $F_1 \otimes F_2$ space as the n, k basis.

The n, k basis vectors may be understood as the superposition of vectors of different n_1 and n_2, but the same n ($\equiv n_1 N_1 + n_2 N_2$) forming eigenvectors of $\hat{T}_{F_1 \otimes F_2}$ (with eigenvalues

[7] Both Ref.'s [18] and [19] consider this analogy, but with quite different and more sophisticated objectives, focusing on incommensurate frequencies and topological aspects.

e^{-ik}):

$$|n,k\rangle_{F_1\otimes F_2} = \frac{1}{\sqrt{N}} \sum_p e^{ipk}\, \hat{T}^p_{F_1\otimes F_2} \, |n_1(n)\rangle_{F_1} \otimes |n_2(n)\rangle_{F_2} \tag{2.27}$$

where for each n we define a *canonical* vector: $|n_1(n)\rangle_{F_1} \otimes |n_2(n)\rangle_{F_2}$ satisfying $n = n_1(n)N_1 + n_2(n)N_2$. One approach to making a specific choice for $n_1(n)$ and $n_2(n)$ is given in Appendix A. The summation may be considered as a limit taken as N, the number of terms in the summation over p, goes to infinity. We do not belabor taking this limit, as it may be avoided, as shown in Appendix B. Imagining the summation as finite is helpful for obtaining an intuitive understanding of the MMFT and SFT equivalence. Furthermore, in Section 2.3.3 we will show that satisfactory numerical implementations of MMFT can be obtained using finite summations over p while preserving the symmetry of the MMFT Hamiltonian given by Eq. 2.26.

In the n, k basis, the final bras in the MMFT propagator of Eq. 2.22 correspond to $k = 0$:

$$\sum_{n_1,n_2} e^{i(n_1\omega_1 + n_2\omega_2)t} \, \langle n_1|_{F_1} \otimes \langle n_2|_{F_2} = \sqrt{N} \sum_n e^{i\omega_B nt} \, \langle n, k=0|_{F_1\otimes F_2} \, . \tag{2.28}$$

The $F_1 \otimes F_2$ part of the initial ket may be written as a superposition of different k vectors:[8]

$$|0\rangle_{F_1} \otimes |0\rangle_{F_2} = \frac{1}{\sqrt{N}} \sum_k |n=0,k\rangle_{F_1\otimes F_2} \, . \tag{2.29}$$

But since $\hat{H}_{F_1\otimes F_2\otimes A}$ does not couple vectors of different k, the final bras dictate that only the $k = 0$ term in the initial ket superposition is relevant, allowing us to write:

$$\begin{aligned} \langle\beta|\, \hat{U}_A(t)\, |\alpha\rangle_A = \sum_n e^{in\omega_B t} \, \big[\langle n, k=0|_{F_1\otimes F_2} \otimes \langle\beta|_A\big] \\ e^{-i\hat{H}_{F_1\otimes F_2\otimes A}t} \, \big[|n=0,k=0\rangle_{F_1\otimes F_2} \otimes |\alpha\rangle_A\big] \, . \end{aligned} \tag{2.30}$$

Thus we see that the part of the spectrum of $\hat{H}_{F_1\otimes F_2\otimes A}$ corresponding to $k \neq 0$ is irrelevant to the propagator. In essence this is the origin of the controversy over MMFT: although the spectrum of $\hat{H}_{F_1\otimes F_2\otimes A}$ contains the appropriate Floquet quasi-energies and states ($k = 0$), it also contains extraneous eigenpairs (corresponding to $k \neq 0$). However, the propagator "selects" the relevant eigenvectors i.e. those corresponding to $k = 0$.

[8] Again we are making use of the convenient fiction that N is finite — in principle the superposition of Eq. 2.29 should be expressed as an integral with k ranging continuously from $-\pi$ to π.

To complete the argument for the correctness of Eq. 2.22, it must be shown that Eq. 2.30 — which is the same as 2.22 but rewritten using the n, k basis — reproduces Shirley's propagator, Eq. 2.14. For this purpose it is sufficient to show that for all possible atomic states specified by γ and ν, and all integer n' and n'''s, the following equality between matrix elements holds:

$$\begin{aligned}\left(\langle n', k=0|_{F_1\otimes F_2} \otimes \langle\gamma|_A\right) \hat{H}_{F_1\otimes F_2\otimes A} \left(|n'', k=0\rangle_{F_1\otimes F_2} \otimes |\nu\rangle_A\right) \\ = \langle n'|_F \otimes \langle\gamma|_A \hat{H}_{F\otimes A} |n''\rangle_F \otimes |\nu\rangle_A .\end{aligned} \tag{2.31}$$

The preceding equality follows from rewriting the $k = 0$ bra and ket of the LHS in the n_1, n_2 basis using Eq. 2.27 and then substituting $\hat{H}_{F_1\otimes F_2\otimes A}$ from Eq. 2.21. We also use

$$\tilde{H}_A(r) = \sum_{p,q} \delta_{r,pN_1+qN_2} \tilde{H}_A(p,q). \tag{2.32}$$

within $\hat{H}_{F\otimes A}$ (from Eq. 2.10) on the RHS of Eq. 2.31.

As the correctness of SFT is well-established, and we have just shown that for commensurate frequencies the MMFT and SFT propagators are equivalent (see also Appendix B), we conclude that usage of the MMFT propagator (Eq. 2.22) is correct for commensurate frequencies.

2.3.2 The significance of the $k \neq 0$ eigenvectors of the MMFT Hamiltonian

Now let us address an objection to the use of MMFT for commensurate frequencies raised by Potvliege and Smith [8], who pointed out that a change in the relative phase of two commensurate fields can be written as a unitary transformation of the MMFT Hamiltonian, and thus its eigenvalues are independent of relative phase (shown below).

This independence seems at odds with experimental observations that the behavior of quantum systems in the presence of external perturbing fields of ω and 2ω depends on the relative phase of the two fields (see, for example, Ref. [31] and the references in Ref. [32]). Our $\omega, 2\omega$ example certainly exhibits this dependence (Fig. 2.1): the time evolution depends strongly on $\phi_{2\omega}$, as do the quasi-energies computed using SFT.

We resolve this apparent paradox by observing that the unitary transformation corresponding to changing the relative phase of the fields is essentially a translation in "k-space", so that a different portion of the spectrum of $\hat{H}_{F_1\otimes F_2\otimes A}$ is "moved" into $k = 0$ (recall that

the propagator only makes use of the $k = 0$ part of the spectrum). Diagonalization of $\hat{H}_{F_1 \otimes F_2 \otimes A}$ may be viewed as a computation of the quasi-energy spectra for *all* phases of the two fields. (In a finite basis this is only approximately realized — a numerical example will be provided in Section 2.3.3.)

To justify the preceding claim, let us consider time-dependent Hamiltonians written in terms of two phases ϕ_1 and ϕ_2:

$$\hat{H}_A(t) = \sum_{p,q} \tilde{H}_A(p,q) e^{ip(\omega_1 t + \phi_1) + iq(\omega_2 t + \phi_2)}, \tag{2.33}$$

which incorporates Eq. 2.17 as a special case. The corresponding MMFT Hamiltonian is:

$$\begin{aligned} \hat{H}_{F_1 \otimes F_2 \otimes A}(\phi_1, \phi_2) = & \sum_{n_1, n_2} [n_1\omega_1 + n_2\omega_2] \, |n_1\rangle \langle n_1|_{F_1} \otimes |n_2\rangle \langle n_2|_{F_2} \otimes \hat{I}_A \\ & + \sum_{p,q} e^{i(p\phi_1 + q\phi_2)} \hat{S}_{F_1}(p) \otimes \hat{S}_{F_2}(q) \otimes \tilde{H}_A(p,q), \end{aligned} \tag{2.34}$$

where we have explicitly indicated the phase-dependence for comparison with the original MMFT Hamiltonian with no phase shifts: $\hat{H}_{F_1 \otimes F_2 \otimes A}(0,0)$.

Defining

$$\hat{U}_F(\phi) \equiv \sum_n e^{-in\phi} \, |n\rangle \langle n|_F \tag{2.35}$$

we may make use of the identity: $e^{ip\phi} \hat{S}_F(p) = \hat{U}_F(\phi)^{-1} \hat{S}_F(p) \hat{U}_F(\phi)$ for F_1 and F_2 in the last term of Eq. 2.34 to write:

$$\begin{aligned} \hat{H}_{F_1 \otimes F_2 \otimes A}(\phi_1, \phi_2) = & \left[\hat{U}_{F_1}(\phi_1)^{-1} \otimes \hat{U}_{F_2}(\phi_2)^{-1} \otimes \hat{I}_A\right] \quad \hat{H}_{F_1 \otimes F_2 \otimes A}(0,0) \\ & \cdot \left[\hat{U}_{F_1}(\phi_1) \otimes \hat{U}_{F_2}(\phi_2) \otimes \hat{I}_A\right], \end{aligned}$$

justifying the claim [8] that a change in the phases of the fields corresponds to a unitary transformation of the MMFT Hamiltonian. As a consequence, given an eigenvector $|\psi\rangle_{F_1 \otimes F_2 \otimes A}$ of $\hat{H}_{F_1 \otimes F_2 \otimes A}(0,0)$, it is also true that $\hat{U}_{F_1}(\phi_1)^{-1} \otimes \hat{U}_{F_2}(\phi_2)^{-1} \otimes \hat{I}_A \, |\psi\rangle_{F_1 \otimes F_2 \otimes A}$ is an eigenvector of $\hat{H}_{F_1 \otimes F_2 \otimes A}(\phi_1, \phi_2)$ with the same eigenvalue.

Using the n, k basis vectors given by Eq. 2.27, together with the convention of Appendix A, we may determine how $\hat{U}_{F_1}(\phi_1)^{-1} \otimes \hat{U}_{F_2}(\phi_2)^{-1}$ effects a shift in k-space:

$$\begin{aligned} \hat{U}_{F_1}(\phi_1)^{-1} \otimes \hat{U}_{F_2}(\phi_2)^{-1} \, |n,k\rangle_{F_1 \otimes F_2} &= e^{i(n_1(n)\phi_1 + n_2(n)\phi_2)} \, |n, k + N_2\phi_1 - N_1\phi_2\rangle_{F_1 \otimes F_2} \\ &= e^{in(n_1(1)\phi_1 + n_2(1)\phi_2)} \, |n, k + N_2\phi_1 - N_1\phi_2\rangle_{F_1 \otimes F_2} \, . \end{aligned} \tag{2.36}$$

Thus, the quasi-energies for non-zero ϕ_1 and ϕ_2 are the eigenvalues of $\hat{H}_{F_1\otimes F_2\otimes A}(0,0)$ corresponding to[9]

$$k = N_1\phi_2 - N_2\phi_1, \tag{2.37}$$

as these $k \neq 0$ eigenvalues of $\hat{H}_{F_1\otimes F_2\otimes A}(0,0)$ correspond to the $k = 0$ eigenvalues of $\hat{H}_{F_1\otimes F_2\otimes A}(\phi_1,\phi_2)$. We will show an example of this correspondence in Section 2.3.3.

Pivotal to the preceding argument has been the point that not all eigenvalues of the MMFT Hamiltonian correspond to quasi-energies (for a fixed set of field phases). Thus the suggestion [7] that for commensurate frequencies the eigenvalues of the MMFT Hamiltonian represent "phase-averaged" quasi-energies is not generally correct. Of course if the eigenvalues are phase-independent then they will be phase averages. The analogous situation for the tight-binding Hamiltonian is that at high-interatomic spacings/low-overlap the energies simply become the atomic energies — different k's are energy degenerate. For MMFT with commensurate frequencies, large N_1 and N_2 and weak couplings will have a similar effect.

2.3.3 Example of the usage of MMFT with retention of translational symmetry (periodic boundary conditions)

Although the $F_1 \otimes F_2$ space used to write two-mode MMFT Hamiltonians is infinite, the example of Section 2.2.3 illustrated that satisfactory numerical solutions for time evolution may be obtained using a truncated basis set for this space — provided it is sufficiently large. However, in a truncated basis set the MMFT Hamiltonian will not typically exhibit the translational symmetry of Eq. 2.26 *exactly*. As such, k may no longer be considered to be a good quantum number of the quasi-states computed by diagonalization of this Hamiltonian.

In this section we show that a judicious selection of a finite set of n_1, n_2 basis vectors, together with the application of periodic boundary conditions — analogous to those used in models of solid-state crystals — preserves the translational symmetry of the MMFT Hamiltonian *exactly* in a finite n_1, n_2 basis. Transforming from this basis to one in which k is a good quantum number block diagonalizes the MMFT Hamiltonian and allows us to illustrate the connection between the $k \neq 0$ eigenpairs and the relative phase of the fields, as discussed in the previous section.

[9] The case of $\phi_1 \neq 0$ and $\phi_2 \neq 0$ but yet $N_2\phi_1 - N_1\phi_2 = 0$ corresponds to an identical time-translation for both fields — the quasi-energies are unchanged and the quasi-states are time-shifted. Equation 2.37 defines what we mean by *relative* phase.

Recall that each n_1, n_2 basis vector has a single associated n ($\equiv n_1 N_1 + n_2 N_2$), but that for a given n there are an infinite number of associated n_1, n_2 vectors (see the discussion surrounding Eq. 2.23). Selection of an appropriate finite basis amounts to deciding which n's will be represented in the basis, and then choosing a finite number of n_1, n_2 vectors for each of these n's (Fig. 2.2(b) provides an example). More specifically, an algorithm for the selection of a finite basis set for $F_1 \otimes F_2$ is:

1. choose a finite set of integers $\mathcal{N}$ specifying the n's that will be represented by the basis. This will typically be the same set as would be used for an equivalent SFT calculation (see Section 2.2.2). For example, $\mathcal{N} = \{n \in \mathbb{Z} \mid n_{\min} \leq n \leq n_{\max}\}$ and in Fig. 2.2(b), $\mathcal{N} = \{-2, -1, 0, 1, 2\}$, corresponding to each diagonal line.

2. for each $n \in \mathcal{N}$ decide on a *canonical* n_1, n_2 basis vector, denoted as $|n_1(n)\rangle_{F_1} \otimes |n_2(n)\rangle_{F_2}$. One way to make this choice is given in Appendix A and an example is shown in Fig. 2.2(b) (using $\otimes$ markers).

3. for each n, generate a set of n_1, n_2 basis vectors by repeated application of $\hat{T}_{F_1 \otimes F_2}$ (see Eq. 2.25) and/or its inverse (both of which preserve n) to the canonical basis vector for this n, giving the basis set: $\mathcal{B}_{F_1 \otimes F_2} = \{\hat{T}^{\ell}_{F_1 \otimes F_2} |n_1(n)\rangle_{F_1} \otimes |n_2(n)\rangle_{F_2} \mid n \in \mathcal{N} \wedge \ell \in \mathcal{L}\}$ where $\mathcal{L} \equiv \{\ell \in \mathbb{Z} \mid \ell_{\min} \leq \ell \leq \ell_{\max}\}$. In Fig. 2.2(b), $\mathcal{L} = \{-2, -1, 0, 1, 2\}$, with each element corresponding to a different location along the diagonals.

The finite basis $\mathcal{B}_{F_1 \otimes F_2}$ generated by the preceding procedure has the following property: given *any* n_1, n_2 basis vector with corresponding $n \in \mathcal{N}$, there always exists one unique integer q such that $(\hat{T}^{N_{\mathcal{L}}}_{F_1 \otimes F_2})^q |n_1\rangle_{F_1} \otimes |n_2\rangle_{F_2}$ is an element of $\mathcal{B}_{F_1 \otimes F_2}$, where $N_{\mathcal{L}}$ is the number of elements in the set $\mathcal{L}$ (if the n_1, n_2 vector is already contained within $\mathcal{B}_{F_1 \otimes F_2}$ then $q = 0$). Each vector within $\mathcal{B}_{F_1 \otimes F_2}$ may be considered as defining an equivalence class containing elements that are not within $\mathcal{B}_{F_1 \otimes F_2}$ (in addition to the vector within $\mathcal{B}_{F_1 \otimes F_2}$).

These equivalences allow periodic boundary conditions to be implemented: if a term in the MMFT Hamiltonian couples a vector n_1, n_2 from $\mathcal{B}_{F_1 \otimes F_2}$ to n_1', n_2', and this vector n_1', n_2' may be "translated" — as described in the previous paragraph — to n_1'', n_2'' within $\mathcal{B}_{F_1 \otimes F_2}$ (always possible if $n_1' N_1 + n_2' N_2 \in \mathcal{N}$), then this coupling is counted as a contribution towards the matrix element between n_1, n_2 and n_1'', n_2''; otherwise it is ignored. Stated in another way: we implement periodic boundary conditions by taking matrix elements of $(\hat{C}_{F_1 \otimes F_2} \otimes I_A) \hat{H}_{F_1 \otimes F_2 \otimes A}$ and $(\hat{C}_{F_1 \otimes F_2} \otimes I_A) \hat{T}_{F_1 \otimes F_2 \otimes A}$ where $\hat{C}_{F_1 \otimes F_2} \equiv \sum_{q \in \mathbb{Z}} (\hat{T}^{N_{\mathcal{L}}}_{F_1 \otimes F_2})^q$. When the finite matrix representations are constructed in this manner, they exhibit the symmetry of Eq. 2.26. In the rest of this section we will refer to $T_{F_1 \otimes F_2 \otimes A}$, $T_{F_1 \otimes F_2}$, and $H_{F_1 \otimes F_2 \otimes A}$

(note no hats) as the finite matrix versions of their operator counterparts with periodic boundary conditions applied.

After $H_{F_1 \otimes F_2 \otimes A}$ has been written in the finite basis formed by combining $\mathcal{B}_{F_1 \otimes F_2}$ with the atomic basis, we may rewrite it in a new basis in which k is a good quantum number. Since $H_{F_1 \otimes F_2 \otimes A}$ does not connect basis vectors of differing k, the Hamiltonian will be block diagonal in this new basis — with each block and its eigenpairs corresponding to a specific k. The new basis may be derived from $\mathcal{B}_{F_1 \otimes F_2}$ using Eq. 2.27, which we can make precise by specifying that the summation is over all $p \in \mathcal{L}$, N is replaced by $N_{\mathcal{L}}$, and $\hat{T}_{F_1 \otimes F_2}$ is replaced by its periodic version. Equation 2.27 then takes the form of a discrete Fourier transform and $T_{F_1 \otimes F_2}$ has eigenvalues uniformly spaced around the unit circle in the complex plane. Following convention, these eigenvalues may be written as e^{-ik} with $k = 2\pi j / N_{\mathcal{L}}$ where j an integer ranging from $-N_{\mathcal{L}}/2$ to $N_{\mathcal{L}}/2 - 1$ if $N_{\mathcal{L}}$ is even, or $-(N_{\mathcal{L}} - 1)/2$ to $(N_{\mathcal{L}} - 1)/2$ if $N_{\mathcal{L}}$ is odd.

We have implemented the preceding procedure for the $\omega, 2\omega$ example discussed in Sections 2.2.2 and 2.2.3. In Fig. 2.1b), the + points represent the eigenvalues of $H_{F_1 \otimes F_2 \otimes A}$, where we have used the correspondence $\phi_{2\omega} = k$ from Eq. 2.37 with $N_1 = 1$, $N_2 = 2$ and $\phi_1 = 0$ suitable for the Hamiltonian of Eq. 2.15. The finite basis used for $F_1 \otimes F_2$ has $N_{\mathcal{L}} = 12$ and $\mathcal{N} = \{-8, -7, \ldots, 8\}$.

Recall that the solid lines of Fig. 2.1(b) correspond to SFT computations with varying $\phi_{2\omega}$ (where the SFT Hamiltonian is constructed and diagonalized for each $\phi_{2\omega}$). By comparison with the + points, we see that diagonalization of a *single* MMFT Hamiltonian samples quasi-energies for a discrete set of relative phases. The spectrum calls to mind the analogy with solid-state crystals: as $N_{\mathcal{L}} \to \infty$ the spectrum of the MMFT Hamiltonian ceases to have isolated eigenvalues, but rather becomes band-like (this property has been previously noted by Potvliege and Smith [8]).

We do not advocate use of the procedure of this section (a special basis set and periodic boundary conditions) for any practical computations, as each k block of the MMFT Hamiltonian is essentially an SFT Hamiltonian corresponding to a certain relative phase. Our purpose in this section was to illustrate with a specific example the connection between the k labelling of eigenpairs of the MMFT Hamiltonian and the phases of the fields.

2.4 Summary and discussion

For commensurate frequencies, the MMFT Hamiltonian has a "translational" symmetry (Eq. 2.26) analogous to that found in tight binding models of solid-state crystals. Using this

symmetry we have established that when applied to time-dependent periodic Hamiltonians involving two commensurate frequencies (of the form given by Eq. 2.20):[10]

1. the MMFT propagator for unitary time evolution (Eq. 2.22) as originally given by Ho *et al.* [5] using the MMFT Hamiltonian (in the modern form of Eq. 2.21) is correct, but

2. not all of the eigenpairs of the MMFT Hamiltonian correspond to the Floquet quasi-energies and quasi-states, and

3. "invalid" eigenpairs of the MMFT Hamiltonian correspond to the quasi-energies and quasi-states for different time-dependent Hamiltonians. These different Hamiltonians correspond to those arising from relative phase shifts of the fields contributing to the Hamiltonian (as detailed in Section 2.3.2 and illustrated by the example of the $\omega, 2\omega$ system in Section 2.3.3).

Although point (1) appears to be a confirmation of Ref. [5], one of the authors of Ref. [5] — following Ref.'s [7] and [8] — later restricted the application of MMFT to incommensurate frequencies, treating the commensurate case using SFT [16] (as we have done in Section 2.2.2 for the $\omega, 2\omega$ example). It appears that authors who reference the original MMFT paper are not always aware of this restriction (partially erroneous because of point (1) and partially correct because of point (2)) and the concerns with the validity of MMFT that have been raised in the literature [7, 8, 6].

Point (2) is important since it is normal (and correct) to take the eigenvalues and eigenstates of Shirley's SFT Hamiltonian (Eq. 2.10) as corresponding to the Floquet quasi-energies and quasi-states, whereas this is not necessarily correct for MMFT. Although one must be slightly cautious when diagonalizing the SFT Hamiltonian within a finite basis, the problematic eigenpairs appear at the extremes of the spectrum. By contrast, as the $\omega, 2\omega$ example of Fig. 2.1b) shows (the X points), erroneous — as they do not correspond to the Floquet quasi-states — eigenpairs of the MMFT Hamiltonian can appear in the centre of the spectrum. Some (in the "bands") correspond (approximately) to different phases of the fields, whereas others (those in the "gaps") are artifacts of basis set truncation.

That some MMFT eigenpairs correspond to the quasi-energies for different relative phases of the fields may be an interesting observation (point (3)), but not necessarily useful. In a finite basis, extra eigenpairs corresponding to differing phases of the fields

[10] Although we have focused on the two-mode case for concreteness, similar conclusions apply to MMFT in cases of more than two modes.

imply a larger matrix representation of the MMFT Hamiltonian than necessary. If one emulates the translational symmetry of the MMFT Hamiltonian (Eq. 2.26) in a finite basis using periodic boundary conditions to allow block diagonalization (as we have done for illustrative purposes in Section 2.3.3), the result is simply equivalent to application of SFT repeatedly for a discrete set of relative phases.

Just as a tight binding Hamiltonian with negligible couplings between lattice sites will produce a set of degenerate atomic energies (the bands collapsing to isolated energies), it is also the case that depending on N_1 and N_2 and the couplings, the approximate diagonalization of MMFT Hamiltonians using finite basis sets may give the correct quasi-energies. In fact, we have not been able to find any examples in the literature where MMFT has given incorrect quasi-energies — presumably because those studies, like the original MMFT paper [5], have concentrated on large N_1 and N_2's, and weak couplings. We are not yet aware of how to state these criteria precisely.

Finally, let us consider MMFT and our results from a modern perspective. Two periodic "dressing" fields can be used to engineer a quantum system, optimizing properties such as low sensitivity to decohering fields [1]. For numerical optimization, the MMFT Hamiltonian has the seemingly(!) attractive property that its structure does not explicitly depend on the precise ratio of the two field frequencies. By contrast, Shirley's formalism is more cumbersome, as the SFT Hamiltonian structure depends on the exact rational representation of the frequency ratio (i.e. N_1 and N_2). If the dressing frequencies are to be varied as part of an optimization process, then the simplicity of MMFT is appealing, but ultimately problematic — optimization may lead to frequency ratios corresponding to low N_1 and N_2. In this context, our $\omega, 2\omega$ example sounds a warning: naive interpretation of the MMFT Hamiltonian eigenenergies as quasi-energies may be incorrect.[11] This warning is despite the correctness of the MMFT propagator (Eq. 2.22) using the same Hamiltonian.

[11] To apply SFT to commensurate multiple frequency problems, the choice of efficient basis sets may still be inspired by MMFT: select *some* of the harmonics of the base frequency using $n = n_1 N_1 + n_2 N_2$, where n_1 and n_2 are small integers, checking for and eliminating(!) any repeated n's.

Chapter 3

Bichromatic dressing of Rydberg atoms

While the dressing of Rydberg atoms with a bichromatic field and low-commensurate frequency components has been studied in the context of phase-dependent ionization [33] and transition probability between bound states [34, 35], there appear to be no studies regarding an induced permanent dipole moment with a bichromatic field.

This chapter focuses on the effect of dressing Rydberg atoms with a linearly polarized bichromatic field of the form

$$\vec{E}(t) = E(t)\hat{e} = \left[E_1 \cos(N_1\omega t + \phi_1) + E_2 \cos(N_2\omega t + \phi_2)\right]\hat{e} \tag{3.1}$$

where $\hat{e}$ is the direction of polarization and N_1 and N_2 are two coprime integers.

In Ref. [36], time-dependent perturbation theory was used to show that a bichromatic field with $N_1 = 1$ and $N_2 = 2$ can induce a permanent dipole moment in an idealized model of an atom. I do not repeat their derivation exactly, as their work primarily focuses on symmetry breaking due to a bichromatic field and on a comparison of the classical and quantum pictures.

Instead, I focus strictly on Rydberg atoms and take an alternative point of view using Floquet theory to show (Section 3.2) that it is possible to induce a permanent dipole moment in a Rydberg atom provided that the following conditions are met:

$$\begin{aligned} &i)\ \text{The sum of } N_1 \text{ and } N_2 \text{ is an odd number}^1 \\ &ii)\ N_1\phi_2 - N_2\phi_1 \neq \frac{\pi}{2} + m\pi, \qquad \{m \in \mathbb{Z}\}. \end{aligned} \tag{3.2}$$

In Section 3.1 I will show that these same conditions lead to a *polar asymmetry* [31] in the bichromatic field. Section 3.2 treats the problem with a Floquet perturbative analysis which shows that there is indeed a non-zero dipole moment if the conditions of Eq. 3.2 are met. I will derive and use a Floquet Hamiltonian for a Rydberg atom in an electric field to determine a set of experimental parameters which can be used to induce a permanent dipole moment in an atom. The results of diagonalizing the Floquet Hamiltonian are shown in Section 3.3.

3.1 Polar asymmetry of a bichromatic dressing field

Certain bichromatic fields can exhibit a property — asymmetry — provided certain conditions are met. This asymmetry suggests the possibility of inducing a permanent dipole moment in an atom as the field now has a "preferred direction" in space. In this section I state precisely the conditions necessary for asymmetry (Figure 3.1 gives examples of asymmetric and symmetric fields). Later, in Section 3.2.2 I show that these same conditions will lead to an induced permanent dipole moment in a Rydberg atom.

To characterize the asymmetry of a function, we can evaluate its n^{th} order moments, where n takes the values of odd, positive integers. Specifically, for the electric field given by Eq. 3.1, its polar asymmetry is characterized by $\langle E^n \rangle$, where $\langle \cdot \rangle$ denotes a time average [31, 37]. By writing a general expression for $\langle E^n \rangle$, it can be shown that if the conditions of Eq. 3.2 are met, then $\langle E^n \rangle \neq 0$ for odd values of $n \geq N_1 + N_2$ and so the electric field is asymmetric.

Starting with Eq. 3.1, $\langle E^n \rangle$ can be written as (with the period, $T = \frac{2\pi}{\omega}$),

$$\langle E^n \rangle = \frac{1}{T} \int_0^T \left[E_1 \cos(N_1 \omega t + \phi_1) + E_2 \cos(N_2 \omega t + \phi_2) \right]^n dt. \tag{3.3}$$

This expression can be rewritten into a useful, albeit awkward form, through the use of

[1] Throughout this text, for any two integers a and b, if their sum is an odd number I will refer to a and b as having *opposite* parities. If their sum is even, then a and b have the *same* parity.

multiple binomial expansions, where $(\cdot)$ is a binomial coefficient,

$$\langle E^n \rangle = \frac{1}{2^n} \sum_{k=0}^{n} \sum_{\ell=0}^{n-k} \sum_{j=0}^{k} \binom{n}{k} \binom{n-k}{\ell} \binom{k}{j} E_1^{n-k} E_2^k \left[e^{i\phi_1(n-k-2\ell)} e^{i\phi_2(k-2j)} \right] \cdot \\ \cdot \frac{1}{T} \int_0^T e^{i\omega t[N_1(n-k-2\ell)+N_2(k-2j)]} dt. \tag{3.4}$$

Despite its complicated form, Eq. 3.4 simplifies greatly by noticing that the integral always evaluates to 0 except where

$$N_1(n-k-2\ell) + N_2(k-2j) = 0, \tag{3.5}$$

in which case it takes the value of T. The solutions to Eq. 3.5 all have the form of

$$\begin{aligned} n-k-2\ell &= \pm A N_2 \\ k-2j &= \mp A N_1 \end{aligned} \tag{3.6}$$

with A equal to 0, or some positive integer where the specific values depend on N_1 and N_2. Note that Eq. 3.4 must be real (since $E(t)$ was real), so if $+A$ is a solution, then $-A$ is as well.

Equations 3.4 - 3.6 allow the following statements to be made, which are slightly rewritten versions of Eq. 3.2. The proofs are simple enough, but are included for completeness:

- $\langle E^n \rangle = 0$ *for all odd* n *when* N_1 *and* N_2 *have the same parity.*

Proof: Assume that the sum of N_1 and N_2 is even, and n is odd. Then, in order to satisfy Eq. 3.5, $(n-k-2\ell)$ and $(k-2j)$ have to have the same parity. Notice that $(n-2\ell)$ is always odd and $(-2j)$ is always even. Adding/subtracting k to both of these results in opposite parities for $(n-k-2\ell)$ and $(k-2j)$. □

- *All nonzero values of* $\langle E^n \rangle$ *for odd* n *are phase dependent, but can be set to 0 when* $N_1\phi_2 - N_2\phi_1 = \pi/2 + m\pi$*, for integer* m*.*

Proof: Only terms where $(n-k-2\ell) = (k-2j) = 0$ are phase independent as the phase factor in Eq. 3.4 is equal to 1. These type of terms never occur at odd n since to satisfy $(k-2j) = 0$, k must be even, which will never satisfy $(n-k-2\ell) = 0$. For all nonzero values of A, the phase factor in Eq. 3.4 is 0 when $N_1\phi_2 - N_2\phi_1 = \pi/2 + m\pi$, for integer m. □

While it is possible to have nonzero $\langle E^n \rangle$ for multiple values of odd n, only one is necessary to show asymmetry, in which case the smallest odd n is likely the simplest and is of interest:

- *The smallest value of odd n for nonzero $\langle E^n \rangle$ is $n = N_1 + N_2$.*

Proof: From Eq. 3.6, $k = \mp A N_1 + 2j$ where A takes the values of positive integers (the case where $A = 0$ does not occur for odd n, as shown above). Since Eq. 3.4 must be real, k must be the same for both $\mp A$ solutions, which indicates that $k \geq N_1$. Similar reasoning shows $n - k \geq N_2$, and so $n \geq N_1 + N_2$. It is easy to see that the equality can always be solved for with $k = N_1$ and $(\ell = 0, j = k)$ or $(\ell = n - k, j = 0)$. □

With $n = N_1 + N_2$, Eq. 3.4 simplifies to

$$\langle E^n \rangle = \frac{1}{2^{n-1}} \binom{n}{N_1} E_1^{N_2} E_2^{N_1} \cos(N_2\phi_1 - N_1\phi_2). \tag{3.7}$$

This is in agreement with Ref. [37], which states this result but does not derive it.

As a specific example, consider the case where $N_1 = 1$ and $N_2 = 2$. In this case, the asymmetry to lowest order can be characterized by the $n = 3$ term,

$$\langle E^3 \rangle = \frac{3}{4} E_1^2 E_2 \cos(2\phi_1 - \phi_2). \tag{3.8}$$

Figure 3.1 illustrates the asymmetry of $E(t)$ with $N_1 = 1$ and $N_2 = 2$. When $2\phi_1 - \phi_2 = \pi/2$, the field is no longer asymmetric. For comparison purposes, $E(t)$ with $N_1 = 1$ and $N_2 = 3$ is shown as these type of fields (N_1 and N_2 have the same parity) never exhibit asymmetry.

In the following section, after introducing the Rydberg Floquet Hamiltonian, I use Floquet theory to show that the permanent dipole moment is non-zero when dressed by a bichromatic field. Specifically, a Floquet perturbative analysis is able to show that the same conditions that lead to the asymmetry of a bichromatic field lead to a permanent dipole moment.

3.2 Inducing a permanent dipole moment with a bichromatic field

A permanent dipole moment induced by the bichromatic field may be detected by applying a small dc electric field and measuring the linear Stark effect on the transition energy between two states. Figure 3.2 shows example Stark shifts with the addition of a permanent dipole moment.

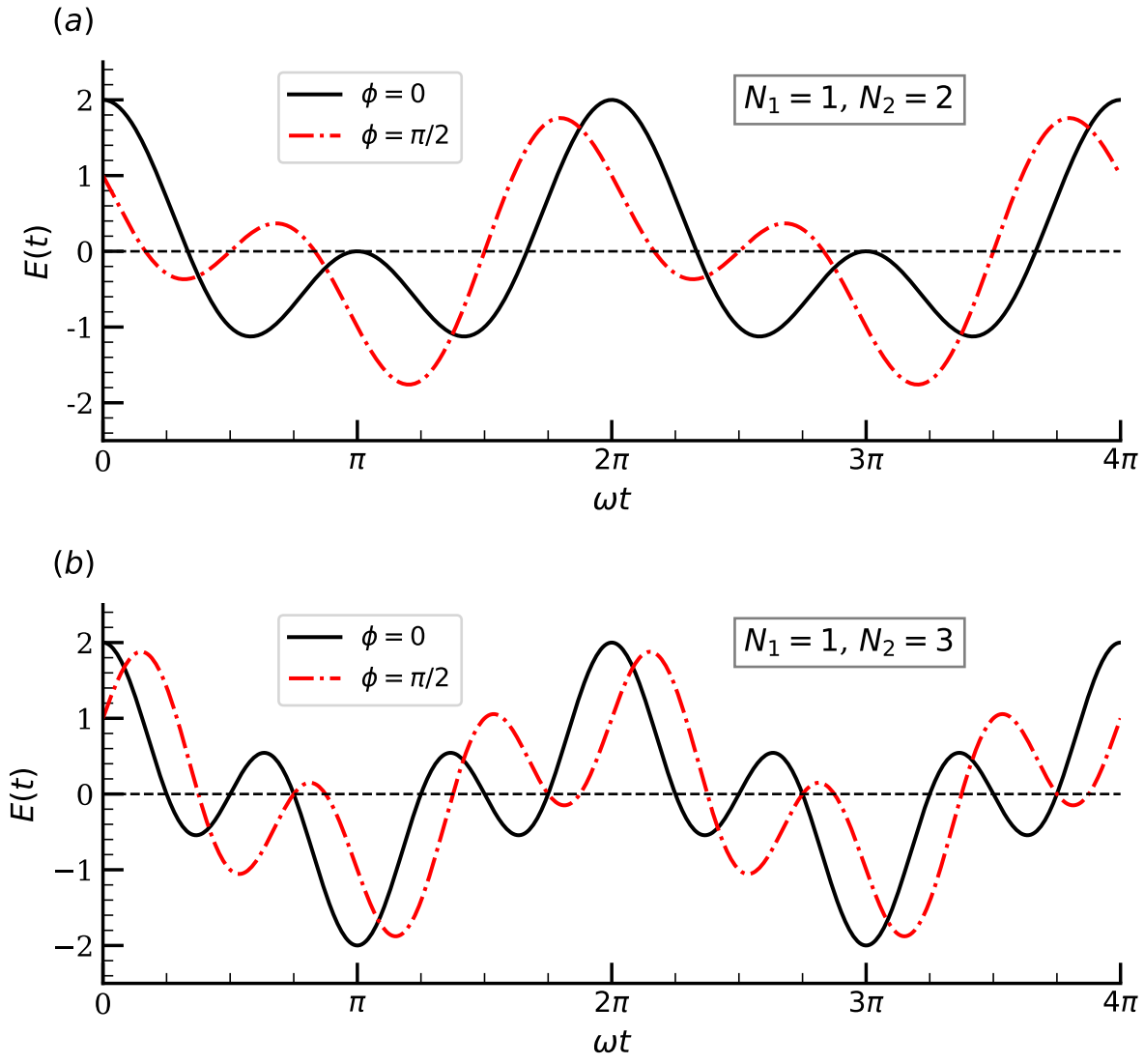

Figure 3.1: Bichromatic fields of the form $E(t) = E_1 \cos(N_1\omega t + \phi_1) + E_2 \cos(N_2\omega t + \phi_2)$ where $E_1 = E_2 = 1$, $\omega = 1$, and $\phi \equiv N_1\phi_2 - N_2\phi_1$. (a) $E(t)$ with $N_1 = 1$, $N_2 = 2$. By adjusting the value of ϕ, the field no longer exhibits asymmetry. (b) $E(t)$ with $N_1 = 1$, $N_2 = 3$. The field never exhibits asymmetry, regardless of the value of ϕ. Two example values of ϕ are shown.

As will be discussed in the following section, in the absence of a permanent dipole moment, the change in energy due to a dc electric field close to 0 V/cm is quadratic, and not linear, in nature (Figure 3.2 (a)). As non-degenerate atomic states do not have their own permanent dipole moment (also discussed below), a permanent dipole moment induced by a bichromatic field will exhibit a linear asymmetry around a zero dc field (Figure 3.2 (b)).

In this section I look only to show that *i*) it is possible to induce a permanent dipole moment in a Rydberg atom using a bichromatic dressing field, and; *ii*) one method of choosing a set of parameters for the set of Rb Rydberg *s*-states. I make no claim that the final choice of parameters is the ideal set, and in fact offer a potentially better method of choosing parameters in Section 3.2.3.

As the Rydberg atom is dressed by a periodic field, the choice of parameters is ultimately determined by diagonalization of Floquet matrices (see Section 2.2.2 for discussion on Floquet theory). In the following section, the Floquet Hamiltonian for a Rydberg atom dressed by a bichromatic field is derived, including discussion on atomic basis and dipole matrix elements.

3.2.1 Floquet Hamiltonian for Rydberg atoms in an electric field

Using the results of Section 2.2.2, I look to derive the Floquet Hamiltonian for a Rydberg atom in both a bichromatic and dc electric field (the dc field is necessary to measure the permanent dipole moment). The corresponding time-dependent Hamiltonian, in the electric dipole approximation, is given by

$$\hat{H}(t) = \hat{H}_0 - \vec{\mu} \cdot [\vec{E}_{dc} + \vec{E}_{ac_1} \cos(N_1 \omega t + \phi_1) + \vec{E}_{ac_2} \cos(N_2 \omega t + \phi_2)] \tag{3.9}$$

where $\hat{H}_0$ is the unperturbed Hamiltonian and $\vec{\mu}$ is the dipole operator.

Rydberg states of alkali metals are highly excited atoms with their valence electron at a large principal quantum number, n. The excited valence electron is largely shielded by the remaining electron core from the electric field due to the nucleus, which results in the valence electron experiencing a Coulombic-like potential; i.e. away from the core, the potential is that of a single, positive charge [38].

If electron spin is ignored, the spherical symmetry indicates that the typical spherical states given by $|nlm_l\rangle$ should be used as the atomic basis. However, for heavier alkali atoms like Rubidium, the fine structure can not be ignored and it is necessary to use the

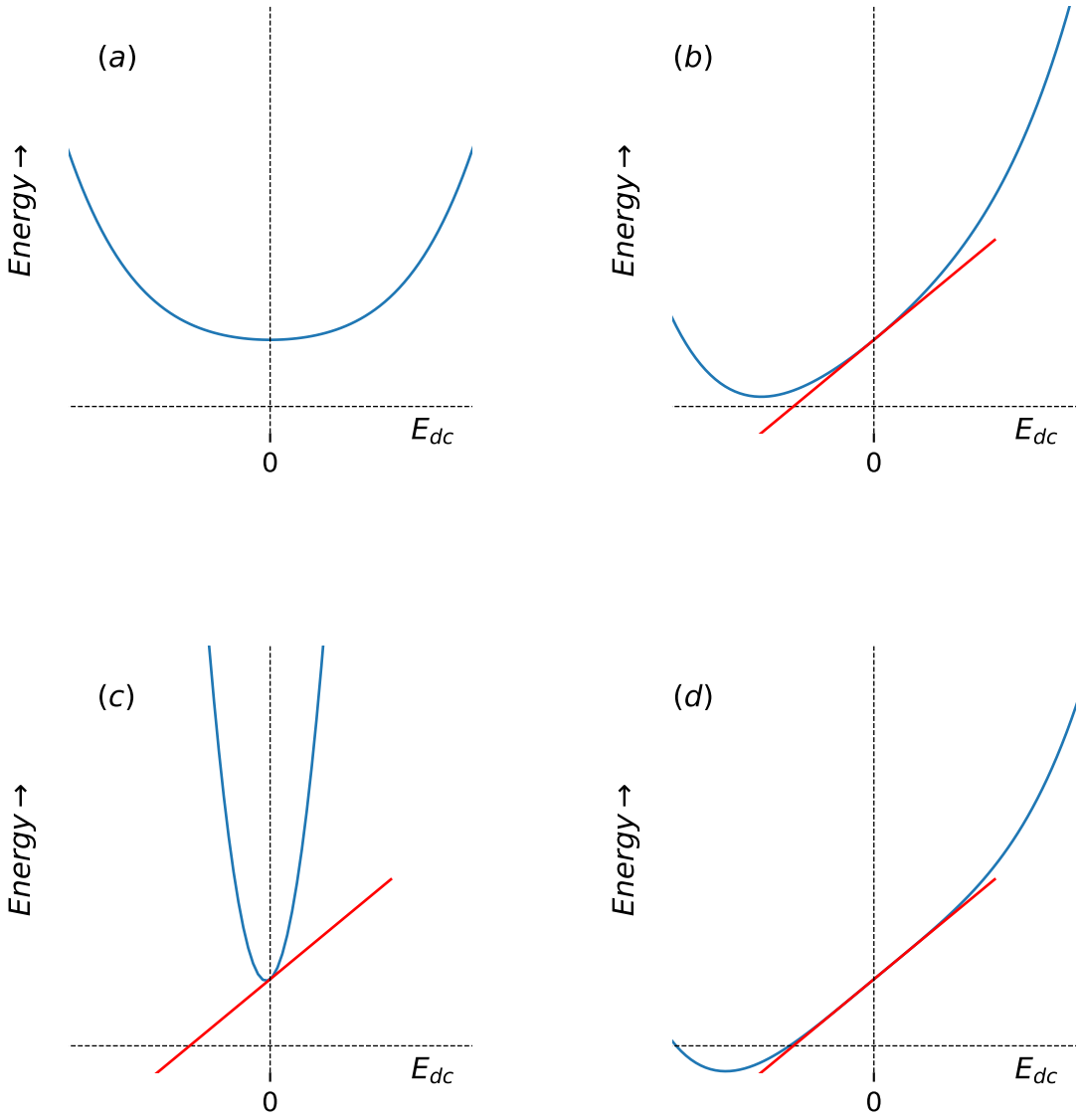

Figure 3.2: Example Stark shifts due to application of a dc electric field (arbitrary units of energy on vertical axis and dc field amplitude on horizontal). The linear Stark effects in (b), (c), and (d) are equivalent. (a) Stark shift with no permanent dipole moment. (b) same plot as (a) with a linear Stark shift added (corresponding to a permanent dipole moment at zero dc electric field). (c) Quadratic Stark effect is too large to reliably measure linear Stark effect (corresponding to a large polarizability). (d) Polarizability nulling. The second order shift is suppressed. Higher order (4th order, for example) effects are still present.

$|nljm_j\rangle$ basis states instead [38]. In this basis, $\hat{H}_0$ is diagonal with elements

$$\langle nljm_j|\hat{H}_0|nljm_j\rangle = \frac{-R_y}{(n-\delta_{nlj})^2} \tag{3.10}$$

where $R_y \approx 13.6$ eV and δ_{nlj} is a quantum defect.

Quantum defects take into account the effects from the finite sized core and are generally empirically observed. In particular, core polarization and core penetration by the valence electron are significant quantum defects which affect the energies of Rydberg states [39, 40].

The dipole matrix elements of Eq. 3.9 are solved for by separating into angular and radial components and are given by [38]

$$\begin{aligned}\langle n'l'j'm'_j|\vec{\mu}|nljm_j\rangle &= e\langle nljm_j|z|nljm_j\rangle \\ &= e\delta_{m_j,m'_j}\delta_{l,l'\pm1}\langle n'l'|r|nl\rangle \\ &\quad\times \sum_{m_l=m_j\pm1/2} C_1(m_l)C_2(m_l)\langle l', m_l|\cos\theta|l, m_l\rangle\end{aligned} \tag{3.11}$$

where the coefficients, $C_1(m_l) = \langle l', \frac{1}{2}, m_j - m_l|j', m_j\rangle$ and $C_2(m_l) = \langle l, \frac{1}{2}, m_l, m_j - m_l|j, m_j\rangle$, are Clebsh-Gordan coefficients. The angular matrix elements $\langle l', m_l|\cos\theta|l, m_l\rangle$ can be calculated algebraically using spherical harmonics, while the radial matrix elements $\langle n'l'|r|nl\rangle$ are typically calculated using numerical integration. Specific information regarding the quantum defects and the calculation of the matrix elements of $\hat{H}(t)$ will be given in Section 3.3.

Given $\hat{H}(t)$ above and using the notation of Chapter 2, the Floquet Hamiltonian is given by

$$\hat{H}_{F\otimes A} = \sum_k \left\{ k\omega|k\rangle\langle k|_F \otimes \hat{I}_A + \sum_m |k+m\rangle\langle k|_F \otimes \tilde{H}_A(m) \right\} \tag{3.12}$$

with $m = 0, \pm N_1, \pm N_2$ and

$$\tilde{H}_A(0) = \sum_\alpha \varepsilon_\alpha|\alpha\rangle\langle\alpha| + \sum_{\alpha\beta} E_{dc}\mu_{\alpha\beta}|\alpha\rangle\langle\beta| \tag{3.13a}$$

$$\tilde{H}_A(\pm N_1) = -\sum_{\alpha\beta} \tfrac{1}{2}E_{ac_1}e^{\pm i\phi_1}\mu_{\alpha\beta}|\alpha\rangle\langle\beta| \tag{3.13b}$$

$$\tilde{H}_A(\pm N_2) = -\sum_{\alpha\beta} \tfrac{1}{2}E_{ac_2}e^{\pm i\phi_2}\mu_{\alpha\beta}|\alpha\rangle\langle\beta| \tag{3.13c}$$

where greek letters represent the atomic states $|nljm_j\rangle$, ε_α is the atomic energy, and $\mu_{\alpha\beta}$ is given by Eq. 3.11.

3.2.2 Floquet perturbation theory

In Section 2.2.2 it was shown that diagonalization of a Floquet Hamiltonian is a non-perturbative method equivalent to solving for the quasienergies of the system. Repeated diagonalization of Eq. 3.12 (in a truncated basis set) over a range of dc field strengths around 0 V/cm will give the quasienergies of the system and show the net Stark effect for a given state.

Nevertheless, this section analyzes the dressing of a Rydberg atom using perturbation theory (PT) in the Floquet picture with the primary reason that PT is able to offer an alternative point of view to what is currently found in the literature regarding inducing a permanent dipole moment with a bichromatic field.

The Rydberg Floquet Hamiltonian from Section 3.2.1 has matrix elements given by (where greek letters still represent the atomic states $|nljm_j\rangle$),

$$\begin{aligned}\langle k'|_F \otimes \langle\beta|_A \hat{H}_{F\otimes A}|k\rangle_F \otimes |\alpha\rangle_A = (\varepsilon_\alpha + k\omega)\delta_{k,k'}\delta_{\alpha,\beta} - \mu_{\alpha,\beta}[E_{dc}\delta_{k,k'} + \\ \tfrac{1}{2}E_{ac_1}e^{\pm i\phi_1}\delta_{k',k\pm N_1} + \tfrac{1}{2}E_{ac_2}e^{\pm i\phi_2}\delta_{k',k\pm N_2}].\end{aligned} \tag{3.14}$$

Here I treat the applied fields as perturbations and use Rayleigh-Schrödinger perturbation theory. Since the atomic basis states (assumed non-degenerate here) are states of definite parity, while the dipole operator has odd parity, only even order perturbative terms are non-zero in a perturbative expansion [41]. For reference, I list the first few general terms of perturbation theory, adopting a similar notation to Ref. [42]:

$$\begin{aligned}\varepsilon_i^{(2)} &= \sum_{i'} \frac{|V_{i,i'}|^2}{\varepsilon_i^{(0)} - \varepsilon_{i'}^{(0)}} \\ \varepsilon_i^{(4)} &= \sum_{i',i'',i'''} \frac{V_{i,i'}V_{i',i''}V_{i'',i'''}V_{i''',i}}{(\varepsilon_i^{(0)} - \varepsilon_{i'}^{(0)})(\varepsilon_i^{(0)} - \varepsilon_{i''}^{(0)})(\varepsilon_i^{(0)} - \varepsilon_{i'''}^{(0)})} \\ &\quad - \sum_{i',i''} \frac{|V_{i,i'}|^2|V_{i,i''}|^2}{(\varepsilon_i^{(0)} - \varepsilon_{i'}^{(0)})(\varepsilon_i^{(0)} - \varepsilon_{i''}^{(0)})^2}\end{aligned} \tag{3.15}$$

where states represented by the index i do not appear in the sums above, and where terms proportional to $V_{i,i}$ have been left out as these terms will be zero for the perturbations given in Eq. 3.14. In general, for each term $\varepsilon_i^{(m)}(\vec{j})$ in an m^{th} order perturbation, we can write

$$\varepsilon_i^{(m)}(\vec{j}) \propto E_{dc}^{j_{dc}} E_{ac_1}^{(j_{ac_1}^+ + j_{ac_1}^-)} E_{ac_2}^{(j_{ac_2}^+ + j_{ac_2}^-)} e^{i\phi_1(j_{ac_1}^+ - j_{ac_1}^-)} e^{i\phi_2(j_{ac_2}^+ - j_{ac_2}^-)} \tag{3.16}$$

where $\vec{j} = (j_{dc}, j^+_{ac_1}, j^-_{ac_1}, j^+_{ac_2}, j^-_{ac_2})$ and where

$$j_{dc} + j^+_{ac_1} + j^-_{ac_1} + j^+_{ac_2} + j^-_{ac_2} = m. \tag{3.17}$$

Each exponent "j" represents the number of times a particular perturbation in Eq. 3.14 is applied. In the Floquet space, each perturbation proportional to $(E_{dc}/E_{ac_1}e^{\pm i\phi_1}/E_{ac_2}e^{\pm i\phi_2})$ will have a corresponding change in Fourier index k by $(0/\pm N_1/\pm N_2)$. For all perturbative expansions, such as in Eq. 3.15, the net change in Fourier index must be zero, i.e.

$$(j^+_{ac_1} - j^-_{ac_1})N_1 + (j^+_{ac_2} - j^-_{ac_2})N_2 = 0. \tag{3.18}$$

This equation is reminiscent of Eq. 3.5, and has solutions of the same form,

$$\begin{aligned} j^+_{ac_1} - j^-_{ac_1} &= \pm BN_2 \\ j^+_{ac_2} - j^-_{ac_2} &= \mp BN_1 \end{aligned} \tag{3.19}$$

where B is an integer greater than or equal to 0 whose possible values depend on N_1 and N_2.

The perturbative terms corresponding to an induced permanent dipole moment are terms which are proportional to E_{dc}. Using similar arguments to those of Section 3.1, it can be shown that these type of terms can only be non-zero when N_1 and N_2 have opposite parities. However, upon substitution of Eq. 3.19 into Eq. 3.16, the real component of all phase dependent terms can be set to zero if $N_1\phi_2 - N_2\phi_1 = \pi/2 + q\pi$, for integer q. As the quasienergies are purely real (the imaginary components cancel each other out when summing up terms of the form of Eq. 3.16), all phase dependent terms can be "turned off" at certain values of relative phase. Thus, as expected, the same conditions from Section 3.1 (Eq. 3.2) that lead to the asymmetry of a bichromatic field lead to an induced permanent dipole moment in an atom.

The strength of the permanent dipole moment can (roughly) be gauged by the lowest non-zero order of perturbation. Again, using the same arguments as in Section 3.1, it can be shown that the lowest non-zero order of a perturbation which induces a permanent dipole moment is $m = N_1 + N_2 + 1$. For this reason, a significant permanent dipole moment can more easily be obtained when the bichromatic field consists of frequencies with a low commensurate ratio. It would seem that the best choice of bichromatic field is one in which $N_1 = 1$ and $N_2 = 2$, and this is what is used in the remainder of this chapter.

3.2.3 Choosing a set of experimental parameters

Between choosing field strengths, frequencies, and which Rydberg state to perform the experiment on, the parameter space is large. To determine which set of parameters is best to

induce a measureable permanent dipole moment, repeated diagonalization of Floquet matrices over a range of dc fields is necessary. This process is simple enough - but lengthy and computationally intensive[2]. In response to this, I offer two strategies which can potentially aid in the choice of experimental parameters.

The first is using a technique called polarizability nulling (discussed below), which relies on Floquet perturbation theory as introduced in the previous section. As this is a perturbative treatment, only in the case of weak fields and frequencies away from atomic resonances will this work. Ultimately, I was not able to use this technique to choose a set of parameters in Rubidium, but I offer it nonetheless as a future reference.

Instead, I use the Hellmann-Feynman theorem [43] to aid in the choice of ω_1, and thus ω_2. In the following sections I will only refer to choosing a single frequency, ω_1, as $\omega_2 = 2\omega_1$ for the remainder of this chapter. Using the Hellmann-Feynman theorem as below is non-perturbative and can always be used as an aid.

Polarizability nulling

While PT makes the decision clear to use $2\omega_1 = \omega_2$, it can also potentially be used as an aid to select possible values of ω_1, and field strengths E_{ac_1} and E_{ac_2}. Using PT up to 4^{th} order, the change in quasienergy of a given state $|k\rangle_F \otimes |\alpha\rangle_A$ due to the linear and quadratic Stark effect is given by

$$\Delta\varepsilon_{\alpha k} \approx \left[C^1_{2,1}(\tfrac{1}{2}E_{ac_1})^2(\tfrac{1}{2}E_{ac_2})\right] E_{dc} + \left[C^2_{0,0} + C^2_{2,0}(\tfrac{1}{2}E_{ac_1})^2 + C^2_{0,2}(\tfrac{1}{2}E_{ac_2})^2\right] E^2_{dc}, \tag{3.20}$$

where the $C^c_{a,b}$'s represent the coefficients of the terms proportional to $(\frac{1}{2}E_{ac_1})^a(\frac{1}{2}E_{ac_1})^b E^c_{dc}$, and, if $a \neq 0$ or $b \neq 0$, are functions of ω_1. Evaluating these coefficients amounts to using the perturbative expressions in Eq. 3.15 with the matrix elements given in Eq. 3.14. There are, in principle, terms that represent ac Stark shifts which I have omitted from Eq. 3.20. The ac Stark shifts are constant over a range of dc fields and only add an overall shift in quasienergy which is not relevant to the discussion in this section. However, when measuring the transition energy between states, it is necessary to be aware of these shifts.

In a perturbative expansion of an energy, the negative of the permanent dipole moment, $-\mu_p$, is the sum of coefficients of the terms proportional to E_{dc}. In Eq. 3.20, there is only one such term, which, to reiterate, is only non-zero because $2\omega_1 = \omega_2$. Thus the permanent dipole moment is only due to the ac fields, and we can let $-\mu_{p,\alpha k} \approx C^1_{2,1}(\frac{1}{2}E_{ac_1})^2(\frac{1}{2}E_{ac_2})$.

[2] As an example, the calculations done for Figure 3.6 in Section 3.3 took ≈ 15 hours to complete on my laptop, which consisted of 55 values of dc field strength over the range considered.

In order to best measure the dipole moment, ideally ω_1 would be chosen such that at least one of $C^2_{2,0}$ or $C^2_{0,2}$ are opposite in sign to $C^2_{0,0}$ so that we can set

$$C^2_{0,0} + C^2_{2,0}(\tfrac{1}{2}E_{ac_1})^2 + C^2_{0,2}(\tfrac{1}{2}E_{ac_2})^2 = 0. \tag{3.21}$$

This is referred to as *polarizability nulling*. (More detailed information regarding polarizability nulling using one field can be found in Ref.'s [44, 45] and using two fields in Ref. [1].) The second order suppression of the dc Stark effect would allow for the easier measurement of the linear Stark effect, and hence, the induced permanent dipole moment (see Figure 3.2 (d)).

It should be noted that PT is only used as an aid to choose parameters for polarizability nulling. Even in non-perturbative regimes polarizability nulling is possible, but requires repeated diagonalization of Floquet matrices over the parameter space (See Ref. [1]). However, I have thus far not been able to determine a set of parameters which satisfy both the polarizability nulling conditions, and which induce a large permanent dipole moment. Given the constraint that the two fields must have frequencies which are low rational ratios of one another, polarizability nulling may not, in general, always be possible. The parameter space is large, however, and I make no claim to having completed an exhaustive search.

In the absence of parameters satisfying Eq. 3.21, I simply look for parameters in which the linear Stark shift is largest *relative* to the quadratic Stark shift (which would otherwise be zero if polarizability nulling was implemented) over a range of dc field strengths close to[3] 0 V/cm. It is not sufficient to have just a large permanent dipole moment, as this can be dominated by a large polarizability (See Figure 3.2 (c)). The set of parameters which consists of the largest relative strength of the linear to quadratic (and higher order) Stark effects is determined by the set of parameters with the best linear fit of the energy plots.

The search involves using values of ω_1 close to atomic resonances, as these generally result in large dipole moments. The large couplings between Rydberg states, as well as being close to resonance, take us out of the perturbative range for the ac field strengths that will be considered. To choose a set of parameters, diagonalization of Floquet matrices is necessary but the Hellmann-Feynman theorem, at the very least, can be used to narrow down the possible choices of ω_1.

[3]Minimum range considered was ≈ 0.2 V/cm away from zero, although a longer range was desirable.

Hellmann-Feynman theorem

While ultimately it is the linear Stark shift relative to the quadratic (and higher order) Stark shifts that are important for measurement, the Hellmann-Feynman theorem [43] can be used to determine the magnitude of the permanent dipole moment. This avoids diagonalizing Floquet matrices over a range of dc field strengths for values of ω_1 which produce negligible permanent dipole moments, regardless of higher order Stark shifts.

If λ is a continuous parameter of a Hamiltonian, $\hat{H}$, then the Hellmann-Feynman theorem states that

$$\frac{d\varepsilon_i}{d\lambda} = \left\langle \psi_i \left| \frac{d\hat{H}}{d\lambda} \right| \psi_i \right\rangle \tag{3.22}$$

where ε_i is the eigenvalue of $\hat{H}$ corresponding to the eigenstate $|\psi_i\rangle$. Applying Eq. 3.22 to the Floquet Hamiltonian (Eq. 3.12) yields the following relationship (note I have dropped the label $F \otimes A$ on the eigenstates for clarity):

$$\frac{d\varepsilon_{\alpha k}}{dE_{dc}} = \left\langle \psi_{\alpha k} \left| \frac{d\hat{H}_{F\otimes A}}{dE_{dc}} \right| \psi_{\alpha k} \right\rangle . \tag{3.23}$$

Here, the eigenstate $|\psi_{\alpha k}\rangle$ represents the dressed state adiabatically[4] connected to the atomic state $|k\rangle_F \otimes |\alpha\rangle_A$.

Taking the derivative of Eq. 3.20 with respect to E_{dc} and evaluating the resulting expression at $E_{dc} = 0$, yields $\frac{d\varepsilon_{\alpha k}}{dE_{dc}}|_{E_{dc}=0} \approx C^1_{2,1}(\frac{1}{2}E_{ac_1})^2(\frac{1}{2}E_{ac_2})$. This expression is approximate as I arbitrarily chose to stop the perturbative expansion at 4^{th} order. Recall however, that the permanent dipole moment is given by the sum of *all* coefficients of terms proportional to E_{dc}. Repeating the process of taking a derivative and setting $E_{dc} = 0$ for a full perturbative expansion of $\varepsilon_{\alpha k}$ results in the following relationship:

$$\frac{d\varepsilon_{\alpha k}}{dE_{dc}}|_{E_{dc}=0} = -\mu_{p,\alpha k}. \tag{3.24}$$

Thus, the Hellmann-Feynman theorem says that

$$\mu_{p,\alpha k} = -\left\langle \psi_{\alpha k} \left| \frac{d\hat{H}_{F\otimes A}}{dE_{dc}} \right| \psi_{\alpha k} \right\rangle_{E_{dc}=0} . \tag{3.25}$$

[4]It may not always be possible to unambiguously define an adiabatically connected state. In these cases, the notation used in this section is inappropriate, but the results hold for any eigenstate regardless.

The permanent dipole moment can be exactly solved for through diagonalization of a Floquet matrix. Implementing Eq. 3.25 computationally involves the following process: *i*) solve for the target eigenstate through diagonalization of $\hat{H}_{F\otimes A}$ with $E_{dc} = 0$, and then; *ii*) take the expectation value of the derivative of $\hat{H}_{F\otimes A}$ using the target eigenstate.

Clearly, in order to solve for the permanent dipole moment for the dressed state $|\psi_{\alpha k}\rangle_{E_{dc}=0}$ using the Hellmann-Feynman theorem as above, the field strengths E_{ac_1} and E_{ac_2} must be chosen. At this point, the exact values are not important — choosing any strengths within the limits set by a particular experiment gives an estimate of the achievable magnitudes of a permanent dipole moment.

Using the Hellmann-Feynman theorem, rather than measuring the linear Stark effect through repeated diagonalization of Floquet matrices, is both quicker and gives a more accurate measurement of the permanent dipole moment. It can easily be repeated for different values of ω_1, indicating which values of ω_1 are suitable to proceed with.

Experimental parameters

After determining which values of ω_1 result in large permanent dipole moments, it is necessary to diagonalize Floquet matrices with various values of E_{ac_1} and E_{ac_2} over a range of dc field strengths to determine the total Stark shift of a given dressed state. The experimental set of parameters is then chosen as the set which results in the best linear fit of the target quasienergy.

I have chosen to dress the $65s_{1/2}$ state of ^{85}Rb with a bichromatic field with $\omega_1/2\pi = 5997$ MHz (and $\omega_2 = 2\omega_1$) and field strengths of $E_{ac_1} = 0.1$ V/cm and $E_{ac_2} = 0.05$ V/cm. The relevant energy level diagram is shown in Figure 3.3. The $65s_{1/2}$ state is coupled to the $63d_{5/2}$ state by a two photon transition consisting of both fields. As a reference, the Stark map for ^{85}Rb $65s_{1/2}$ and $64s_{1/2}$ is shown in Figure 3.4, while Figure 3.5 focuses strictly on the Stark map for $65s_{1/2}$.

Up until this point, the preceding discussion has focused on the Stark effect of a single dressed state. However, the practical way to test these results is measuring the Stark effect on the transition energy between two states. I choose to measure the transition energy between the $64s_{1/2}$ and the $65s_{1/2}$ dressed states. While the $64s_{1/2}$ state does not exhibit large ac Stark shifts, it still has a sizeable dc Stark Shift (see Figure 3.7 in Section 3.3). While this is not ideal, the permanent dipole moment induced in the $65s_{1/2}$ is still prevalent. If necessary however, mitigating this problem in the future involves making a transition from a different state which does not have large ac or dc Stark shifts (possibly

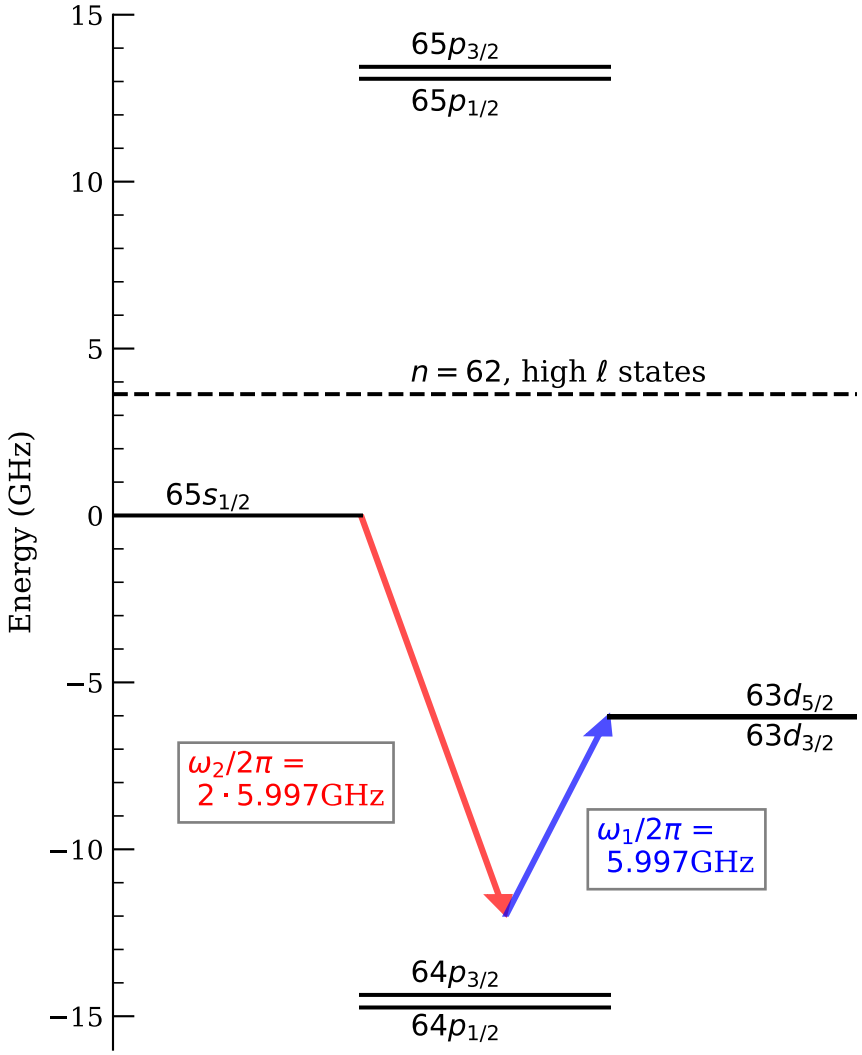

Figure 3.3: Energy level diagram for ^{85}Rb $65s_{1/2}$. The $65s_{1/2}$ state is coupled through a two photon transition to the $63d_{5/2}$ state. The combined two-photon process is off-resonance by 10MHz. The $63d_{5/2}$ and $63d_{3/2}$ states are not resolved in this diagram. For reference the energy of the ^{85}Rb, $n = 62$ high angular momentum states are shown (these have hydrogen-like energies).

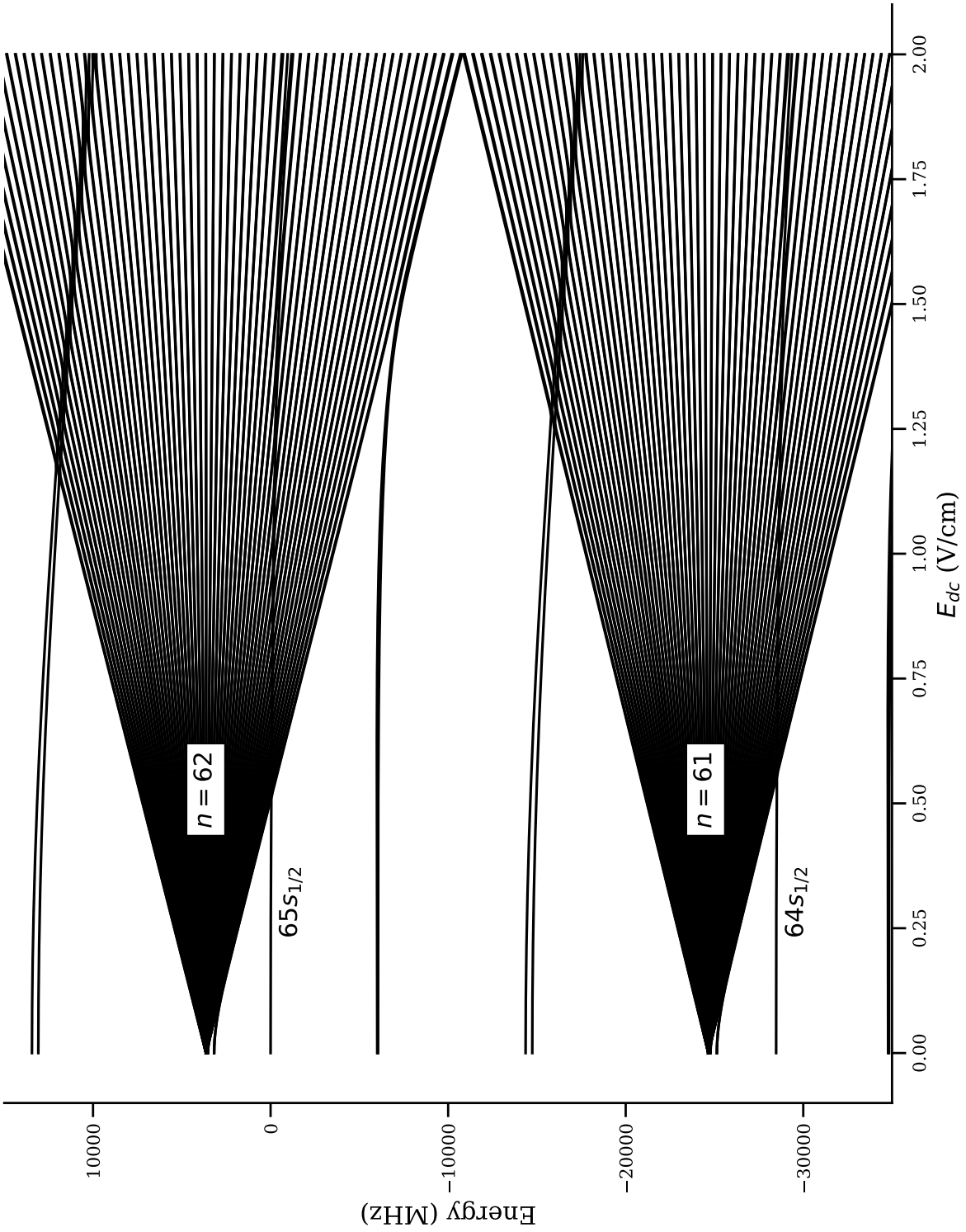

Figure 3.4: Dc Stark map for ^{85}Rb $65s_{1/2}$ and $64s_{1/2}$. The $65s_{1/2}$ state joins the $n = 62$ manifold at ≈ 0.51 V/cm and the $64s_{1/2}$ joins the $n = 61$ manifold at ≈ 0.55 V/cm. This plot does not include any effects from the bichromatic dressing field.

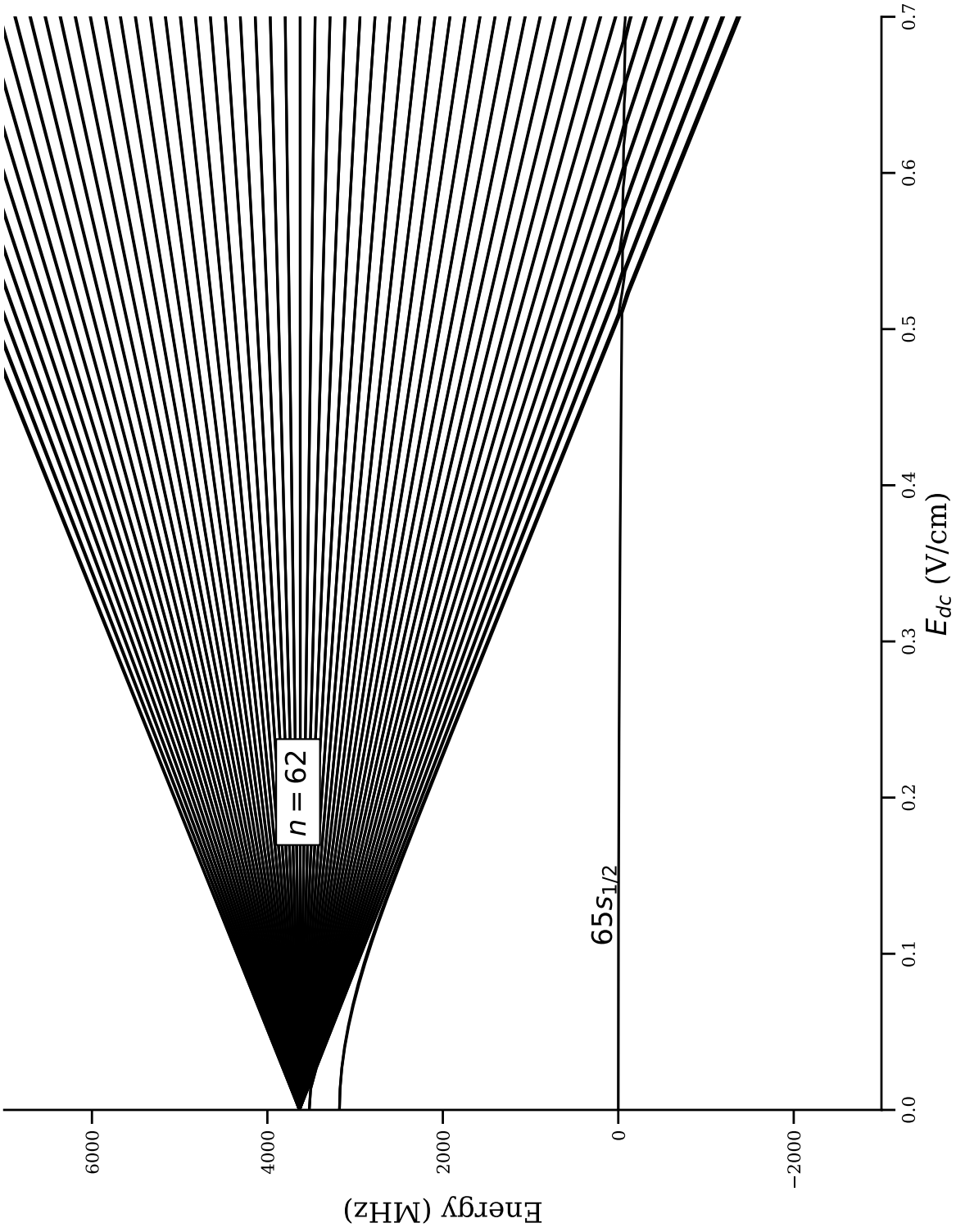

Figure 3.5: Zoomed in region of Figure 3.4 to focus on dc Stark map for ^{85}Rb $65s_{1/2}$.

ground state), or using the polarizability nulling method on the transition energy rather than the energy of a single state.

Nonetheless, for the purposes of this paper, the transition between the dressed states of $64s_{1/2}$ and $65s_{1/2}$ of ^{85}Rb is sufficient. The results of the following section illustrate the effects of dressing these Rydberg states with the bichromatic field above, both by plotting the quasienergies of the states individually, and by plotting their transition energy.

3.3 Results

The quasienergy plots from this section were results of diagonalizing Floquet matrices (Eq. 3.12) over dc field strengths ranging from -0.35 V/cm to 0.35 V/cm with frequencies $\omega_1/2\pi = 5997$ MHz, $\omega_2 = 2\omega_1$, and field strengths $E_{ac_1} = 0.1$ V/cm, $E_{ac_2} = 0.05$ V/cm. Outside of this range of dc fields, the spectrum for the dressed $65s_{1/2}$ state becomes rather complicated, undergoing multiple avoided crossings. Analyzing this part of the spectrum is outside the scope of this work.

The Floquet basis was chosen to include 863 atomic states (closest in energy to the $65s_{1/2}$ state of Rubidium), and 13 Floquet side bands ($n = -6\omega_1, -5\omega_1, \ldots, 5\omega_1, 6\omega_1$). For all quasienergy plots in this section, increasing the number of Floquet sidebands had a negligible difference, while at 863 atomic states the quasienergies had converged to within 0.5%.

The Floquet matrix elements were calculated using the Alkali Rydberg Calculator (ARC) [46]. ARC uses atomic energies retrieved from the NIST ASD database [47] or calculated from known quantum defects (for Rubidium see Ref.'s [48, 49, 50]). Dipole matrix elements are calculated as in Section 3.2.1 using Eq. 3.11 with the radial matrix elements calculated through numerical integration using the Numerov technique (see, for example, [38]).

For both the $65s_{1/2}$ and $64s_{1/2}$ states, $m_j = 1/2$, and the value of ϕ refers to the relative phase between the fields, and is defined (as before) as $\phi = N_1\phi_2 - N_2\phi_1$.

Dressed ^{85}Rb $65s_{1/2}$

Figure 3.6 shows the result of dressing the $65s_{1/2}, m_j = 1/2$ state with a bichromatic field. Two dressed states are shown which have significant dependencies on $65s_{1/2}$.

When $\phi = 0$, the permanent dipole moment is at a maximum and the linear Stark effect is clearly illustrated in the upper dressed state at dc field strengths ranging from roughly

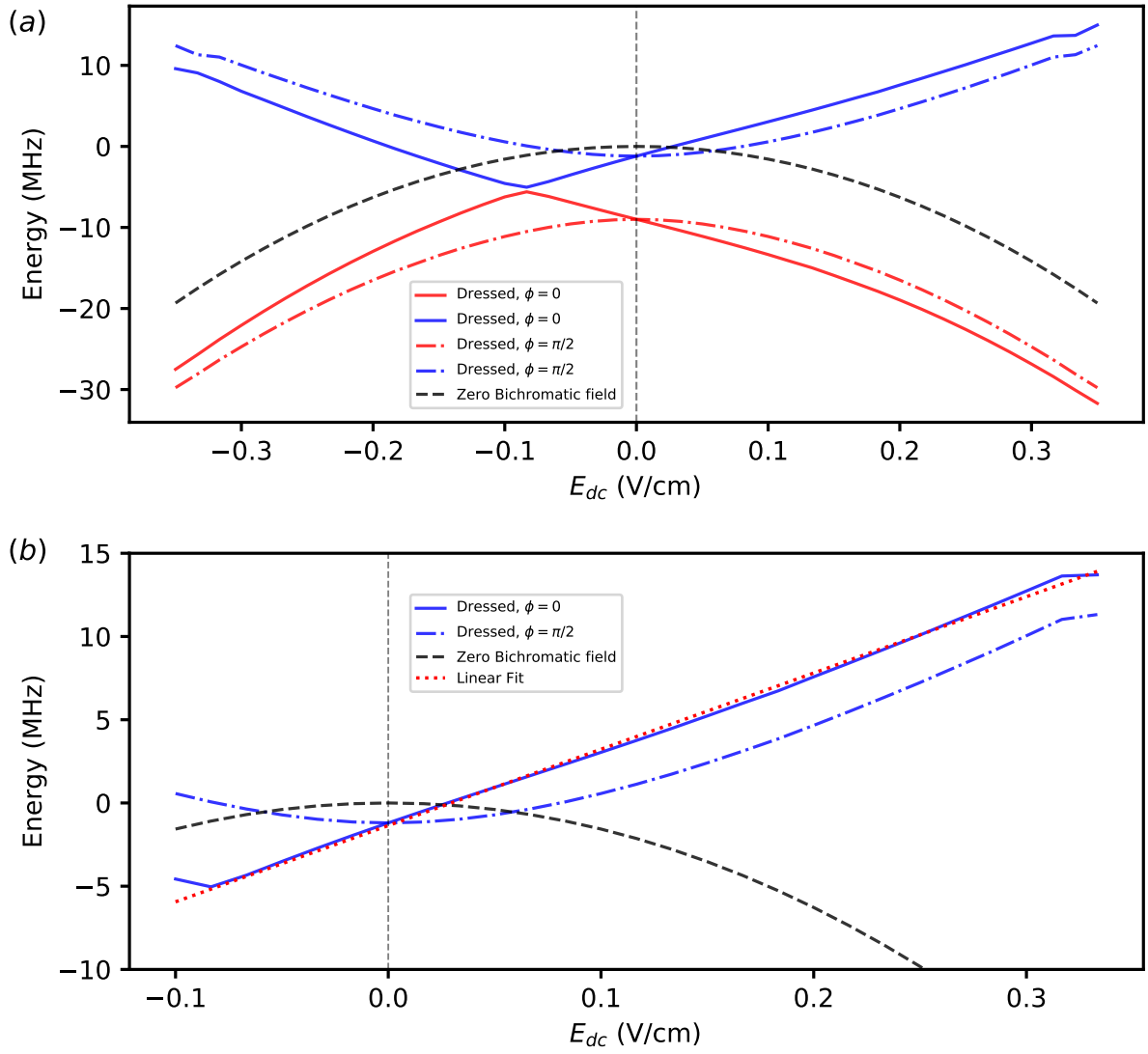

Figure 3.6: Quasienergy plot of dressed $65s_{1/2}$ state of ^{85}Rb with $\omega_1 = 2\pi \cdot 5997$ MHz, $\omega_2 = 2\omega_1$, $E_{ac_1} = 0.1$ V/cm, $E_{ac_2} = 0.05$ V/cm. Zero in energy corresponds to the atomic ^{85}Rb $65s_{1/2}$ state. (a) E_{dc} ranging from -0.35 V/cm to 0.35 V/cm. Two quasistates with significant dependency on $65s_{1/2}$ are shown at different values of field phases: $\phi = 0$, where the permanent dipole moment is maximal, and $\phi = \pi/2$ where there is no permanent dipole moment. The zero-ac field $65s_{1/2}$ state is shown for reference. (b) Zoomed in region of (a) to illustrate linear Stark shift, focused on dc strengths ranging from -0.1 V/cm to 0.3 V/cm. A linear fit to the quasienergy has been added with slope equal to 45.82 MHz/(V/cm).

Table 3.1: Comparison of electric dipole moments of various atoms and molecules. Figure 3.5 illustrates the dipole moments given in rows two and three in this table. PbO was chosen as it posseses an average sized dipole moment relative to other common molecules [51].

	electric dipole moment
Dressed ^{85}Rb $65s_{1/2}$	$34.4ea_0$
^{85}Rb $65s_{1/2}$ before joining $n = 62$ Stark manifold	$\sim 120ea_0$
Upper state in $n = 62$ ^{85}Rb Stark manifold	$\sim 5590ea_0$
^{85}Rb $65s_{1/2}$ as a classical dipole	$\sim 3830ea_0$
PbO molecule	$1.06ea_0$

-0.1 V/cm to 0.3 V/cm. The linear fit of the quasienergy in this region gives a slope (which $= -\mu_p$) of 45.82 MHz/(V/cm) which is in good agreement with the value calculated using the Hellmann-Feynman theorem, which gives a value of $\mu_p = -44.06$ MHz/(V/cm). The two dressed states approach in energy, however, and undergo an avoided crossing (differ by < 1 MHz) at $E_{dc} \approx -0.08$ V/cm.

At $\phi = \pi/2$ the permanent dipole moment is 0 and the dressed states show no linear Stark effect — the energy is perfectly symmetric around $E_{dc} = 0$ V/cm. This indicates that the permanent dipole moment can be controlled by adjusting the relative value of the phase between the two ac fields. The permanent dipole moment can take intermediate values (not shown here) between zero and -44.06 MHz/(V/cm) by adjusting ϕ to values between 0 and $\pi/2$, and can in fact change sign for values of ϕ betwen $\pi/2$ and π.

Table 3.1 shows a comparison of dipole moment strengths between various atoms and molecules in units of ea_0 where e is the elementary charge and a_0 is the Bohr radius. See Figure 3.5 for a plot of the ^{85}Rb $n = 62$ Stark manifold. It should also be noted that the parameters which were selected to induce a permanent dipole moment in ^{85}Rb $65s_{1/2}$ were intended to give the largest permanent dipole moment *relative* to higher order Stark effects, and not to induce the largest permanent dipole moment in magnitude. The magnitude of the permanent dipole moment of the dressed ^{85}Rb $65s_{1/2}$ can be increased by increasing the bichromatic field strengths.

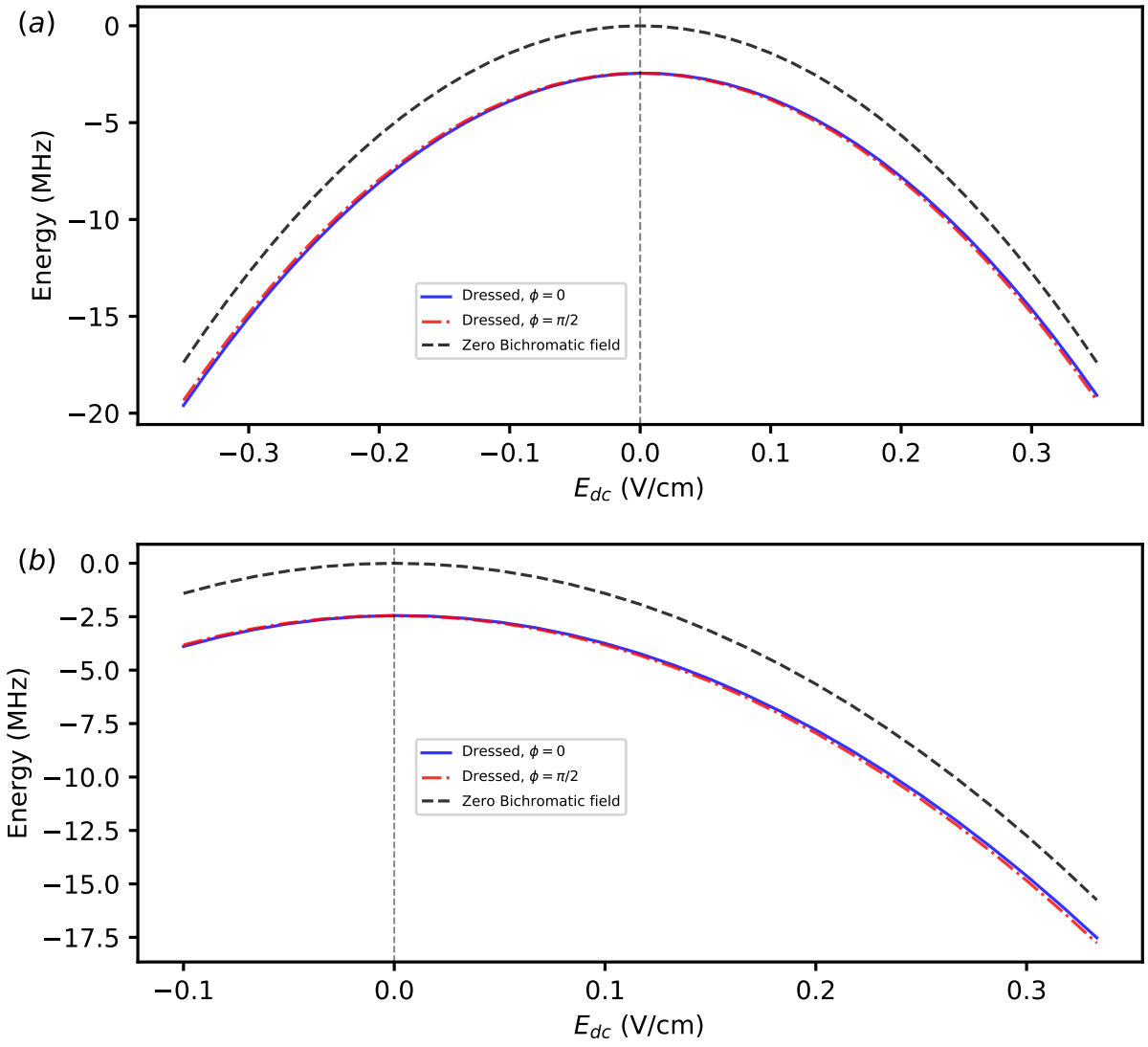

Figure 3.7: Quasienergy plot of dressed $64s_{1/2}$ state of ^{85}Rb with $\omega_1 = 2\pi \cdot 5997$ MHz, $\omega_2 = 2\omega_1$, $E_{ac_1} = 0.1$ V/cm, $E_{ac_2} = 0.05$ V/cm. Zero in energy corresponds to the atomic ^{85}Rb $64s_{1/2}$ state. (a) E_{dc} ranging from -0.35 V/cm to 0.35 V/cm. There is only a single relevant quasistate which is adiabatically connected to the $64s_{1/2}$ state. Changing the value of ϕ has little effect. The zero-ac field $64s_{1/2}$ state is shown for reference. (b) Zoomed in region of (a) focused on dc strengths ranging from -0.1 V/cm to 0.3 V/cm.

Dressed ^{85}Rb $64s_{1/2}$

The dressed $64s_{1/2}$ state of ^{85}Rb was chosen as the final state in the transition necessary to measure the effect of the bichromatic field. Figure 3.7 shows the quasienergy plot for the state adiabatically connected to $64s_{1/2}$.

The bichromatic field has only a small effect on the quasienergy, resulting in an ac Stark shift of ∼3MHz. The quasienergies for $\phi = 0$ and $\phi = \pi/2$ differ marginally, indicating that there is a slight permanent dipole moment induced in this state as well. For reference, the Hellmann-Feynman theorem gives a value for the permanent dipole moment of -0.72 MHz/(V/cm). The dc Stark shift is on the order of ∼30MHz over the range considered, which is significant. However, as will be shown, this is still not large enough to dominate the transition — the permanent dipole moment induced in the $65s_{1/2}$ quasistate is still measurable.

^{85}Rb $65s_{1/2} \rightarrow 64s_{1/2}$ transition

Figure 3.8 shows the transition energy between the upper quasistate in Figure 3.6 and the $64s_{1/2}$ adiabat. Despite the large dc Stark shift in the $64s_{1/2}$ adiabat, the permanent dipole moment is still a large effect and is particularly prevalent around $E_{dc} = 0$ V/cm. A comparison with $\phi = \pi/2$ clearly illustrates the asymmetry of the linear Stark effect due to the permanent dipole moment.

The results of this section illustrate that a bichromatic field is able to induce a measureable permanent dipole moment in a Rydberg state of Rubidium. However, it is still unclear if and how this work can be improved (possibly by polarizability nulling). Possible improvements and other potential work regarding related aspects to these results are discussed in the following section.

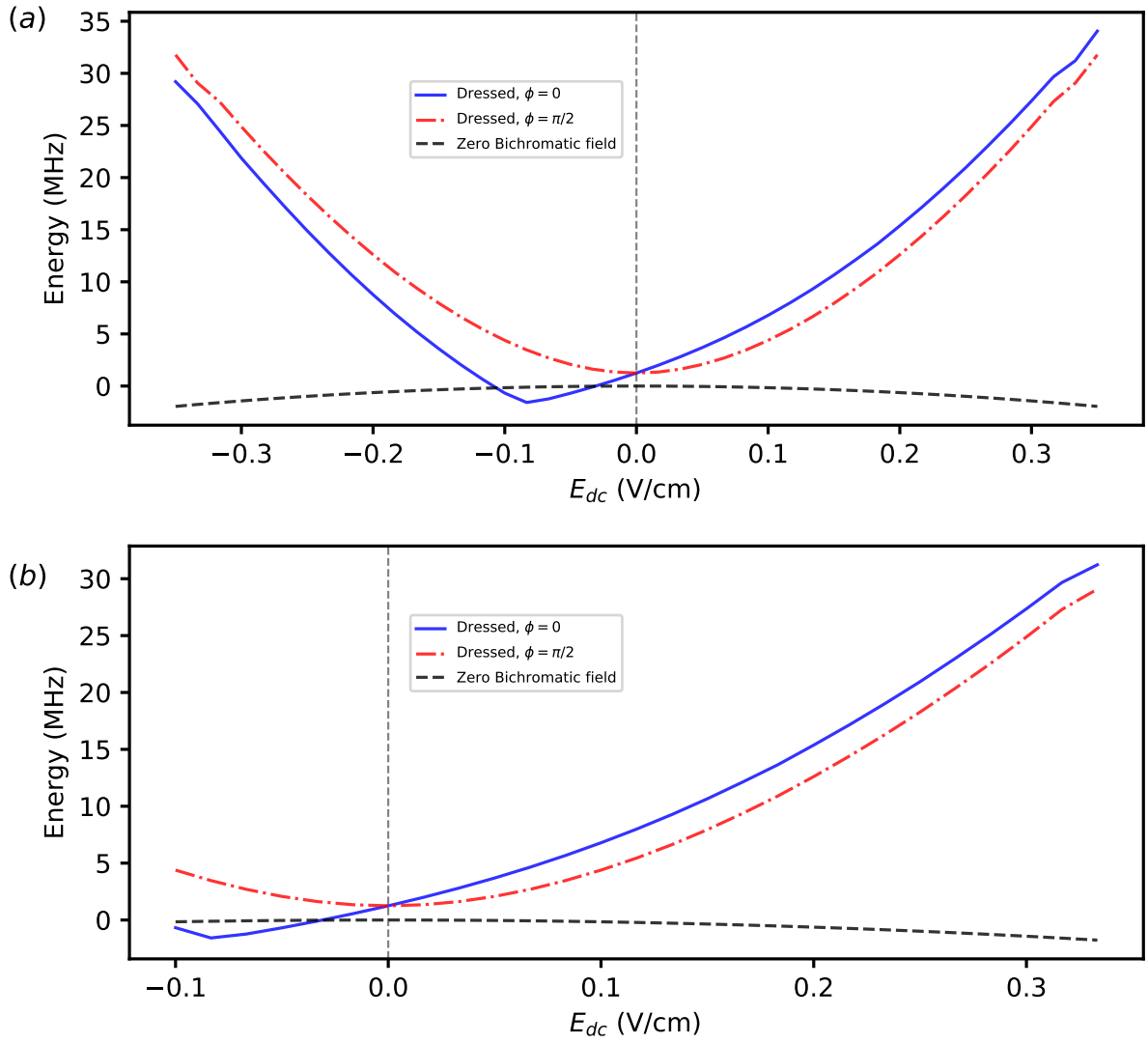

Figure 3.8: Transition energy between the $64s_{1/2}$ quasistate and the upper $65s_{1/2}$ quasistate (see Figure 3.6), dressed with a bichromatic field with $\omega_1 = 2\pi \cdot 5997$ MHz, $\omega_2 = 2\omega_1$, $E_{ac_1} = 0.1$ V/cm, $E_{ac_2} = 0.05$ V/cm. The difference in atomic energy between $65s_{1/2}$ and $64s_{1/2}$ (≈ 28.472 GHz) is subtracted off. The abrupt change in transition energy at -0.08 V/cm is due to the avoided crossing present in Figure 3.6. (a) E_{dc} ranging from -0.35 V/cm to 0.35 V/cm. The zero-ac field transition energy is shown for reference. (b) Zoomed in region of (a) focused on dc strengths ranging from -0.1 V/cm to 0.3 V/cm.

Chapter 4

Conclusions and future work

In Chapter 2, I clear up confusion in the literature [6, 7, 8] regarding MMFT using commensurate frequencies. I show that MMFT always reproduces the time-evolution of a system exactly, despite having only part of its eigenvalue spectrum directly correspond to time evolution. I show that the rest of the eigenvalue spectrum corresponds to the same system, but at *different* values of the relative phase ($\phi = N_1\phi_2 - N_2\phi_1$) between the two ac fields.

However, despite the correctness of MMFT (if used appropriately), Floquet theory is always recommended in the case of commensurate frequencies. Unless the symmetry of MMFT is taken advantage of (as in Section 2.3.3), diagonalizing MMFT matrices gives extraneous eigenvalues which are not of interest. Taking advantage of the translational symmetry avoids the extraneous eigenvalues, but results in diagonalization of the same Hamiltonian as in Floquet theory anyway, and so is also not recommended.

While I feel that MMFT in the case of commensurate frequencies is now well understood, future work regarding MMFT may include analyzing the situation of incommensurate frequencies. While there is work on this topic [18, 19], the original MMFT derivation relies on the fact that the frequencies are commensurate. This indicates that there is possible area for improvement — at the very least in the derivation of MMFT.

Using Floquet theory, I have shown that a bichromatic field can induce a permanent electric dipole moment (first order energy shift due to a dc electric field) in an atom, provided that N_1 and N_2 have opposite parities (where $N_1 = \omega_1/\omega$ and $N_2 = \omega_2/\omega$ and ω_1, ω_2 are the frequency components of the bichromatic field). With the aid of the Hellmann-Feynman theorem, parameters suitable for inducing a measurable permanent dipole moment in a Rubidium Rydberg state were selected.

Specifically, Floquet calculations were performed which show that a bichromatic field with frequencies $\omega_1/2\pi = 5997$ MHz, $\omega_2 = 2\omega_1$ and field strengths $E_{ac_1} = 0.1$ V/cm, $E_{ac_2} = 0.05$ V/cm are able to induce a permanent dipole moment in the dressed $65s_{1/2}$ state of ^{85}Rb with a maximal magnitude of 44.06 MHz/(V/cm). The permanent dipole moment is phase dependent and is able to be set to zero at a relative phase value $\phi = \pi/2$. That a bichromatic field can induce a permanent dipole moment without a dc electric field may potentially be beneficial to neutral atom qubits [2, 3] which rely on strong dipole-dipole interactions, particularly by offering the ability to more quickly turn on and control the permanent dipole moment.

The bichromatic field couples the $65s_{1/2}$ state to the $63d_{5/2}$ state through a two photon transition. It is expected that the necessary parameters needed to induce a permanent dipole moment (frequencies and field strengths) scale reliably with the value of the principal quantum number n. Inducing a permanent dipole moment in a different $ns_{1/2}$ state should be possible by coupling it to an $(n-2)d_{5/2}$ state through a two photon transition, provided that the necessary ac field strengths do not become too large. At the moment, it is also unclear if this particular coupling will work in other Rydberg atoms (other alkali metals), so calculations should be performed in this regard as well. All calculations should be verified experimentally.

Using a technique called polarizability nulling, there is opportunity to search for improved parameters which allow for easier measurement of the linear Stark effect (and thus the permanent dipole moment) through a reduction in the quadratic Stark effect.

References

[1] D. W. Booth, J. Isaacs, and M. Saffman, "Reducing the sensitivity of Rydberg atoms to dc electric fields using two-frequency ac field dressing," *Phys. Rev. A*, vol. 97, p. 012515, Jan. 2018.

[2] M. Saffman, T. G. Walker, and K. Mølmer, "Quantum information with Rydberg atoms," *Reviews of Modern Physics*, vol. 82, pp. 2313–2363, Aug. 2010.

[3] M. Saffman, "Quantum computing with atomic qubits and Rydberg interactions: Progress and challenges," *Journal of Physics B: Atomic, Molecular and Optical Physics*, vol. 49, no. 20, p. 202001, 2016.

[4] M. D. Lukin, M. Fleischhauer, R. Cote, L. M. Duan, D. Jaksch, J. I. Cirac, and P. Zoller, "Dipole Blockade and Quantum Information Processing in Mesoscopic Atomic Ensembles," *Physical Review Letters*, vol. 87, p. 037901, June 2001.

[5] T.-S. Ho, S.-I. Chu, and J. V. Tietz, "Semiclassical many-mode floquet theory," *Chem. Phys. Lett.*, vol. 96, pp. 464–471, Apr. 1983.

[6] A. Verdeny, J. Puig, and F. Mintert, "Quasi-Periodically Driven Quantum Systems," *Z. Für Naturforschung A*, vol. 71, pp. 897–907, Jan. 2016.

[7] M. Dörr, R. M. Potvliege, D. Proulx, and R. Shakeshaft, "Multiphoton processes in an intense laser field. VI. Two-color ionization with incommensurable frequencies," *Phys. Rev. A*, vol. 44, pp. 574–583, July 1991.

[8] R. M. Potvliege and P. H. G. Smith, "Two-colour multiphoton ionization of hydrogen by an intense laser field and one of its harmonics," *J. Phys. B: At. Mol. Opt. Phys.*, vol. 25, pp. 2501–2516, June 1992.

[9] J. H. Shirley, "Solution of the Schrödinger Equation with a Hamiltonian Periodic in Time," *Phys. Rev.*, vol. 138, pp. B979–B987, May 1965.

[10] A. K. Mohapatra, T. R. Jackson, and C. S. Adams, "Coherent Optical Detection of Highly Excited Rydberg States Using Electromagnetically Induced Transparency," *Physical Review Letters*, vol. 98, p. 113003, Mar. 2007.

[11] A. N. Poertner and J. D. D. Martin, "On the validity of many-mode Floquet theory with commensurate frequencies," *arXiv:1912.02770 [physics, physics:quant-ph]*, Dec. 2019.

[12] W. van de Water, S. Yoakum, T. van Leeuwen, B. E. Sauer, L. Moorman, E. J. Galvez, D. R. Mariani, and P. M. Koch, "Microwave multiphoton ionization and excitation of helium Rydberg atoms," *Phys. Rev. A*, vol. 42, pp. 572–591, July 1990.

[13] M. Leskes, P. K. Madhu, and S. Vega, "Floquet theory in solid-state nuclear magnetic resonance," *Prog. NMR Spectrosc.*, vol. 57, pp. 345–380, Nov. 2010.

[14] A. Chakraborty and S. R. Mishra, "A Floquet formalism for the interaction of magnetically trapped atoms with rf fields," *J. Phys. B-At. Mol. Opt. Phys.*, vol. 51, p. 025002, Jan. 2018.

[15] M. Sameti and M. J. Hartmann, "Floquet engineering in superconducting circuits: From arbitrary spin-spin interactions to the Kitaev honeycomb model," *Phys. Rev. A*, vol. 99, p. 012333, Jan. 2019.

[16] D. A. Telnov, J. Wang, and S.-I. Chu, "Above-threshold multiphoton detachment of H^- by two-color laser fields: Angular distributions and partial rates," *Physical Review A*, vol. 51, pp. 4797–4808, June 1995.

[17] S.-I. Chu and D. A. Telnov, "Beyond the Floquet theorem: Generalized Floquet formalisms and quasienergy methods for atomic and molecular multiphoton processes in intense laser fields," *Phys. Rep.*, vol. 390, pp. 1–131, Feb. 2004.

[18] I. Martin, G. Refael, and B. Halperin, "Topological Frequency Conversion in Strongly Driven Quantum Systems," *Phys. Rev. X*, vol. 7, p. 041008, Oct. 2017.

[19] P. J. D. Crowley, I. Martin, and A. Chandran, "Topological classification of quasiperiodically driven quantum systems," *Phys. Rev. B*, vol. 99, p. 064306, Feb. 2019.

[20] G. Birkhoff and G.-C. Rota, *Ordinary Differential Equations*. New York: Wiley, 4th ed ed., 1989.

[21] M. Holthaus, "Floquet engineering with quasienergy bands of periodically driven optical lattices," *J. Phys. B At. Mol. Opt. Phys.*, vol. 49, p. 013001, Jan. 2016.

[22] S. Leasure and R. Wyatt, "Floquet theory of the interaction of a molecule with a laser field - techniques and an application," *Opt. Eng.*, vol. 19, no. 1, pp. 46–56, 1980.

[23] B. Deconinck and J. Nathan Kutz, "Computing spectra of linear operators using the Floquet–Fourier–Hill method," *J. Comput. Phys.*, vol. 219, pp. 296–321, Nov. 2006.

[24] S. H. Autler and C. H. Townes, "Stark Effect in Rapidly Varying Fields," *Phys. Rev.*, vol. 100, pp. 703–722, Oct. 1955.

[25] H. Sambe, "Steady states and quasienergies of a quantum-mechanical system in an oscillating field," *Phys. Rev. A*, vol. 7, no. 6, pp. 2203–2213, 1973.

[26] S. P. Goreslavskii and V. P. Krainov, "Two-level atom in a bichromatic resonance field," *Sov. Phys. JETP*, vol. 49, p. 13, 1979.

[27] S. Leasure, "An approach to laser—molecule dynamics using raising and lowering operators," *Chem. Phys.*, vol. 67, pp. 83–95, May 1982.

[28] K. H. Rosen, *Elementary Number Theory and Its Applications*. Boston: Pearson/Addison Wesley, 5th ed., 2005.

[29] N. W. Ashcroft and N. D. Mermin, *Solid State Physics*. New York: Holt, Rinehart and Winston, 1976.

[30] J. C. Garrison, "Quantum mechanics of periodic systems," *Am. J. Phys.*, vol. 67, pp. 196–203, Feb. 1999.

[31] N. B. Baranova, A. N. Chudinov, and B. Y. Zel'dovich, "Polar asymmetry of photoionization by a field with $\langle E3 \rangle \neq 0$. Theory and experiment," *Opt. Commun.*, vol. 79, pp. 116–120, Oct. 1990.

[32] M. Shapiro and P. Brumer, *Quantum Control of Molecular Processes*. Weinheim: Wiley-VCH, 2nd, rev. and enl. ed ed., 2012.

[33] L. Sirko and P. M. Koch, "Control of Common Resonances in Bichromatically Driven Hydrogen Atoms," *Physical Review Letters*, vol. 89, Dec. 2002.

[34] L. Ko, M. W. Noel, J. Lambert, and T. F. Gallagher, "Two-mode multiphoton transitions," *Journal of Physics B: Atomic, Molecular and Optical Physics*, vol. 32, pp. 3469–3483, July 1999.

[35] L. Sirko, S. A. Zelazny, and P. M. Koch, "Use of the Relative Phase in a Bichromatic Field Pulse to Control a Quasienergy Gap," *Physical Review Letters*, vol. 87, p. 043002, July 2001.

[36] I. Franco and P. Brumer, "Laser-Induced Spatial Symmetry Breaking in Quantum and Classical Mechanics," *Physical Review Letters*, vol. 97, July 2006.

[37] V. A. Pazdzersky and V. I. Usachenko, "The interference phenomena at negative ion photodecay in a bichromatic field," *Journal of Physics B: Atomic, Molecular and Optical Physics*, vol. 30, pp. 3387–3402, Aug. 1997.

[38] M. L. Zimmerman, M. G. Littman, M. M. Kash, and D. Kleppner, "Stark structure of the Rydberg states of alkali-metal atoms," *Physical Review A*, vol. 20, pp. 2251–2275, Dec. 1979.

[39] R. R. Freeman and D. Kleppner, "Core polarization and quantum defects in high-angular-momentum states of alkali atoms," *Physical Review A*, vol. 14, pp. 1614–1619, Nov. 1976.

[40] M. J. Seaton, "Quantum defect theory," *Reports on Progress in Physics*, vol. 46, pp. 167–257, Feb. 1983.

[41] A. Khadjavi, A. Lurio, and W. Happer, "Stark Effect in the Excited States of Rb, Cs, Cd, and Hg," *Physical Review*, vol. 167, pp. 128–135, Mar. 1968.

[42] L. D. Landau and E. M. Lifshitz, *Quantum Mechanics: Non-Relativistic Theory (3rd Ed.)*. Pergamon Press Ltd., 1977.

[43] R. P. Feynman, "Forces in Molecules," *Physical Review*, vol. 56, pp. 340–343, Aug. 1939.

[44] L. A. Jones, J. D. Carter, and J. D. D. Martin, "Rydberg atoms with a reduced sensitivity to dc and low-frequency electric fields," *Physical Review A*, vol. 87, p. 023423, Feb. 2013.

[45] Y. Ni, P. Xu, and J. D. D. Martin, "Reduction of the dc-electric-field sensitivity of circular Rydberg states using nonresonant dressing fields," *Physical Review A*, vol. 92, p. 063418, Dec. 2015.

[46] N. Šibalić, J. D. Pritchard, C. S. Adams, and K. J. Weatherill, "ARC: An open-source library for calculating properties of alkali Rydberg atoms," *Computer Physics Communications*, vol. 220, pp. 319–331, Nov. 2017.

[47] Alexander Kramida, Y. Ralchenko, and J. Reader, "NIST Atomic Spectra Database." https://www.nist.gov/pml/atomic-spectra-database, July 2009.

[48] W. Li, I. Mourachko, M. W. Noel, and T. F. Gallagher, "Millimeter-wave spectroscopy of cold Rb Rydberg atoms in a magneto-optical trap: Quantum defects of the ns, np, and nd series," *Physical Review A*, vol. 67, p. 052502, May 2003.

[49] J. Han, Y. Jamil, D. V. L. Norum, P. J. Tanner, and T. F. Gallagher, "Rb nf quantum defects from millimeter-wave spectroscopy of cold ^{85}Rb rydberg atoms," *Physical Review A*, vol. 74, p. 054502, Nov. 2006.

[50] K. Afrousheh, P. Bohlouli-Zanjani, J. A. Petrus, and J. D. D. Martin, "Determination of the ^{85}Rb ng-series quantum defect by electric-field-induced resonant energy transfer between cold rydberg atoms," *Physical Review A*, vol. 74, p. 062712, Dec. 2006.

[51] S. C. Wright, T. E. Wall, and M. R. Tarbutt, "Microwave trap for atoms and molecules," *Physical Review Research*, vol. 1, p. 033035, Oct. 2019.

[52] S. A. Rankin, "The Euclidean Algorithm and the Linear Diophantine Equation ax + by = gcd(a, b)," *Am. Math. Mon.*, vol. 120, no. 6, pp. 562–564, 2013.

APPENDICES

Appendix A

Choice of canonical n_1, n_2

In the main text, we have referred at points (e.g. Eq. 2.27) to vectors: $|n_1(n)\rangle_{F_1} \otimes |n_2(n)\rangle_{F_2}$, specific to each n, satisfying $n_1(n)N_1 + n_2(n)N_2 = n$. Here we describe a method to select these vectors. i.e. how to choose n_1 and n_2 for a given n (the functional dependence on N_1 and N_2 is left implicit in our notation).

The extended Euclidean algorithm (EEA) (see for example Ref. [28]) simultaneously determines both the greatest common divisor (gcd) of two positive integers a and b and a specific integer solution for x and y satisfying $ax + by = \gcd(a, b)$. Since for any given rational frequency ratio we may always choose N_1 and N_2 so that $\gcd(N_1, N_2) = 1$, we use the EEA to solve for $n_1(1)$ and $n_2(1)$ satisfying

$$n_1(1)N_1 + n_2(1)N_2 = 1 \tag{A.1}$$

(and also verify that $\gcd(N_1, N_2) = 1$). Multiplying both sides of Eq. A.1 by n suggests that we define: $n_1(n) \equiv n_1(1)n$ and $n_2(n) \equiv n_2(1)n$. This choice is used in Fig. 2.2(b) and in the numerical example of Section 2.3.3.

Reference [52] points out that the EEA produces an integer solution for x and y to $ax+by = \gcd(a, b)$ having minimal x^2+y^2, which is desirable for the aesthetics of Fig. 2.2(b), but by no means necessary.

Appendix B

Justification of the MMFT propagator without basis set truncation

In the main text, the equivalence of the MMFT propagator (Eq. 2.22) to Shirley's Floquet propagator (Eq. 2.14) for commensurate frequencies is demonstrated using physically suggestive summations over a finite number of n_1, n_2 basis vectors to produce n, k vectors. Here we justify the equivalence of the propagators in a more rigorous manner.

The MMFT propagator (Eq. 2.22) can be written in a form resembling the SFT propagator through the introduction of two linear maps: 1) a "promotion" map P from $F \otimes A$ to $F_1 \otimes F_2 \otimes A$, and 2) a "demotion" map D from $F_1 \otimes F_2 \otimes A$ to $F \otimes A$:

$$\langle\beta|\,\hat{U}_A(t)\,|\alpha\rangle = \sum_n e^{in\omega_B t}\,\langle n|_F \otimes \langle\beta|_A \; D\, e^{-i\hat{H}_{F_1\otimes F_2\otimes A}t}\; P\,|0\rangle_F \otimes |\alpha\rangle_A\,, \tag{B.1}$$

with

$$D \equiv \sum_{n_1,n_2} |n_1 N_1 + n_2 N_2\rangle_F\,\langle n_1|_{F_1} \otimes \langle n_2|_{F_2} \otimes \hat{I}_A, \tag{B.2}$$

and

$$P \equiv \sum_n |n_1(n)\rangle_{F_1} \otimes |n_2(n)\rangle_{F_2}\,\langle n|_F \otimes \hat{I}_A, \tag{B.3}$$

where $n_1(n)N_1 + n_2(n)N_2 = n$ (see Appendix A; the choice of P is not unique and nor is it required to be). Note that although

$$DP = \hat{I}_{F\otimes A}, \tag{B.4}$$

we have:

$$PD \neq \hat{I}_{F_1 \otimes F_2 \otimes A}, \tag{B.5}$$

since mapping from $F_1 \otimes F_2 \to F$ "loses" information i.e. it is possible that $D\left|n_1\right\rangle_{F_1} \otimes \left|n_2\right\rangle_{F_2} = D\left|n_1'\right\rangle_{F_1} \otimes \left|n_2'\right\rangle_{F_2}$ with $n_1 \neq n_1'$ or $n_2 \neq n_2'$. Applying P to map back into $F_1 \otimes F_2$ does not restore this information.

Comparison of the MMFT propagator written using D and P (Eq. B.1) to the SFT propagator (Eq. 2.14) shows that their equivalence will follow if

$$\hat{H}^j_{F \otimes A} = D\hat{H}^j_{F_1 \otimes F_2 \otimes A}P \tag{B.6}$$

for all non-negative integer j. The $j = 0$ case follows from Eq. B.4. For $j > 0$ it is sufficient that

$$\hat{H}_{F \otimes A}D = D\hat{H}_{F_1 \otimes F_2 \otimes A}, \tag{B.7}$$

since by acting with P from the right on both sides (and using Eq. B.4) we have

$$\hat{H}_{F \otimes A} = D\hat{H}_{F_1 \otimes F_2 \otimes A}P, \tag{B.8}$$

and subsequently acting from the left of both sides with $H_{F \otimes A}$ and using B.7 to simplify the RHS gives Eq. B.6 for $j = 2$. This process may be continued to establish Eq. B.6 for any positive integer j.

To show Eq. B.7 we take $\hat{H}_{F_1 \otimes F_1 \otimes A}$ from Eq. 2.21, and $\hat{H}_{F \otimes A}$ as given by Eq. 2.10, making use of Eq. 2.32 to ensure that both SFT and MMFT Hamiltonians refer to the same time-dependent Hamiltonian in the atomic space. This establishes the equivalence of the MMFT propagator (Eq. 2.22) to Shirley's Floquet propagator (Eq. 2.14).